International Institute for
Applied Systems Analysis
www.iiasa.ac.at

Evolutionary-branching lines and areas in bivariate trait spaces

Ito, H.C. and Dieckmann, U.

IIASA Interim Report
2012

Interim Report   **IR-12-043**

Evolutionary-branching lines and areas in bivariate trait spaces

Hiroshi C. Ito
Ulf Dieckmann (dieckmann@iiasa.ac.at)

Approved by

Pavel Kabat
Director General and Chief Executive Officer

February 2015

Evolutionary-branching lines and areas in bivariate trait spaces

Hiroshi C. Ito[1] and Ulf Dieckmann[1]

[1]*Evolution and Ecology Program, International Institute for Applied Systems Analysis,*

Schlossplatz 1, A-2361 Laxenburg, Austria

E-mail addresses: H. C. Ito, hiroshibeetle@gmail.com; U. Dieckmann, dieckmann@iiasa.ac.at

ABSTRACT

Aims: Evolutionary branching is a process of evolutionary diversification induced by frequency-dependent ecological interaction. Here we show how to predict the occurrence of evolutionary branching in bivariate traits when populations are evolving directionally.

Methods: Following adaptive dynamics theory, we assume low mutation rates and small mutational step sizes. On this basis, we generalize conditions for evolutionary-branching points to conditions for evolutionary-branching lines and areas, which delineate regions of trait space in which evolutionary branching can be expected despite populations still evolving directionally along these lines and within these areas. To assess the quality of predictions provided by our new conditions for evolutionary branching lines and areas, we analyse three eco-evolutionary models with bivariate trait spaces, comparing the predicted evolutionary-branching lines and areas with actual occurrences of evolutionary branching in numerically calculated evolutionary dynamics. In the three examples, a phenotype's fitness is affected by frequency-dependent resource competition and/or predator–prey interaction.

Conclusions: In the limit of infinitesimal mutational step sizes, evolutionary branching in bivariate trait spaces can occur only at evolutionary-branching points, i.e., where the evolving population experiences disruptive selection in the absence of any directional selection. In contrast, when mutational step sizes are finite, evolutionary branching can occur also along evolutionary-branching lines, i.e., where disruptive selection orthogonal to these lines is sufficiently strong relative to directional selection along them. Moreover, such evolutionary-branching lines are embedded in evolutionary-branching areas, which delineate all bivariate trait combinations for which evolutionary branching can occur when mutation rates are low,

while mutational step sizes are finite. Our analyses show that evolutionary-branching lines

and areas are good indicators of evolutionary branching in directionally evolving populations.

We also demonstrate that not all evolutionary-branching lines and areas contain evolutionary-

branching points, so evolutionary branching is possible even in trait spaces that contain no

evolutionary-branching point at all.

INTRODUCTION

Evolutionary branching is a process of evolutionary diversification induced by ecological in-

teraction (Metz *et al.*, 1992; Geritz *et al.*, 1997, 1998; Dieckmann *et al.*, 2004), which can

occur through all fundamental types of ecological interaction, including competition, preda-

tor-prey interaction, and mutualism (Doebeli and Dieckmann, 2000; Dieckmann *et al.*, 2007).

Therefore, evolutionary branching may be an important mechanism underlying the sympatric

or parapatric speciation of sexual populations driven by frequency-dependent selection pres-

sures (e.g., Doebeli, 1996; Dieckmann and Doebeli, 1999; Kisdi and Geritz, 1999; Doebeli

and Dieckmann, 2003; Dieckmann *et al.*, 2004; Claessen *et al.*, 2008; Durinx and Van Door-

en, 2009; Heinz *et al.*, 2009; Payne *et al.*, 2011).

In asexual populations with rare and small mutational steps, evolutionary branching oc-

curs through trait-substitution sequences caused by the sequential invasion of successful mu-

tants. In univariate trait spaces, a necessary and sufficient condition for evolutionary branch-

ing is the existence of a convergence stable trait value, called an evolutionary-branching

point, at which directional selection is absent and the remaining selection is locally disruptive

(Metz *et al.*, 1992; Geritz *et al.*, 1997).

Real populations, however, have undergone, and are usually undergoing, evolution in

many quantitative traits, with large variation in their evolutionary speeds (e.g., Hendry and

Kinnison, 1999; Kinnison and Hendry, 2001). Such speed differences among traits may be

due to smaller mutation rates and/or magnitudes in some traits than in others, and will also

arise when fitness is less sensitive to some traits than to others.

Only a few previous studies have analytically investigated evolutionary branching in mul-

tivariate trait spaces (Ackermann and Doebeli, 2004; Egas *et al.*, 2005; Leimar, 2005; Ravi-

gné *et al.*, 2009). Those studies assumed that all considered traits evolve at comparable speeds, and analyzed possibilities of evolutionary branching by examining the existence of evolutionary-branching points having the following four properties: evolutionary singularity (no directional selection), convergence stability (local evolutionary attractor for monomorphic evolution), evolutionary instability (locally disruptive selection), and mutual invasibility (local coexistence of dimorphic trait values). All of these studies have therefore considered the vanishing of directional selection as a prerequisite for evolutionary branching.

On the other hand, Ito and Dieckmann (2007) have numerically shown that, when mutational step sizes are not infinitesimal, evolutionary branching can occur even in directionally evolving populations, as long as directional evolution is sufficiently slow. This implies that trait spaces may contain evolutionary-branching lines that attract monomorphic evolution and then induce evolutionary branching while populations are directionally evolving along them. Furthermore, Ito and Dieckmann (submitted) derived sufficient conditions for the existence of such evolutionary-branching lines, by focusing on trait-substitution sequences formed by invasions each of which possesses maximum likelihood, called maximum-likelihood invasion paths (MLIPs).

In this study, we heuristically extend the derived sufficient conditions for evolutionary-branching lines to sufficient conditions for evolutionary-branching areas, and apply these two sets of conditions to three eco-evolutionary models with bivariate trait spaces. Our study is structured as follows. The next section explains conditions for evolutionary-branching lines and extends those to evolutionary-branching areas. In the first example, we apply the two sets of conditions to a resource-competition model with two evolving niche positions. In the second example, we show their application to another resource-competition model with evolving niche position and niche width. In the third example, a predator-prey model with two evolving niche positions is analyzed. The last section discusses how our conditions improve understanding of evolutionary branching in multivariate trait spaces.

1 **CONDITIONS FOR EVOLUTIONARY-BRANCHING LINES AND AREAS**

2 In this section, we review and explain the sufficient conditions for evolutionary-branching

3 lines (Ito and Dieckmann, submitted) and extend them to evolutionary-branching areas. We

4 consider bivariate trait spaces spanned by two scalar traits X and Y, denoted by

5 $\mathbf{S} = (X,Y)^{\mathrm{T}}$ (where T denotes transposition). The conditions for evolutionary-branching

6 lines and areas are analyzed by introducing a locally normalized coordinate system

7 $\mathbf{s} = (x,y)^{\mathrm{T}}$ at each point of the original coordinate system $\mathbf{S} = (X,Y)^{\mathrm{T}}$. Throughout this pa-

8 per, all model definitions, figures, and verbal discussions of the models are presented in terms

9 of the original coordinate systems, while the analytic conditions, e.g., in Eqs. (1-3), are pre-

10 sented using the locally normalized coordinate systems.

11 **Local normalization of invasion-fitness function**

12 We consider an asexual monomorphic population in an arbitrary bivariate trait space

13 $\mathbf{S} = (X,Y)^{\mathrm{T}}$. Throughout this study, we assume low mutation rates and small mutational step

14 sizes. Under the former assumption, the population is almost always close to population-

15 dynamical equilibrium when a mutant emerges. It can then also be shown that, in the absence

16 of population-dynamical bifurcations and when mutational step sizes are not only small, but

17 infinitesimal, the population remains monomorphic in the course of directional evolution

18 (Geritz *et al.*, 2002): under these conditions, a mutant phenotype $\mathbf{S}'$ can invade and replace a

19 resident phenotype $\mathbf{S}$ if its invasion fitness is positive, resulting in what is called a trait sub-

20 stitution.

21 The invasion fitness of $\mathbf{S}'$ under $\mathbf{S}$, denoted by $F(\mathbf{S}';\mathbf{S})$, is defined as the exponential

22 growth rate of a small population of phenotypes $\mathbf{S}'$ in the environment created by a mono-

23 morphic population of phenotypes $\mathbf{S}$ at its population-dynamical equilibrium (Metz *et al.*,

24 1992). The invasion-fitness function F can be interpreted as a fitness landscape in $\mathbf{S}'$,

25 whose shape depends on $\mathbf{S}$. For small mutational step sizes, repeated invasion and replace-

26 ment of $\mathbf{S}$ by $\mathbf{S}'$ in the direction of the fitness gradient $\partial F(\mathbf{S}';\mathbf{S})/\partial \mathbf{S}'|_{\mathbf{S}'=\mathbf{S}}$ brings about a

27 trait-substitution sequence, resulting in gradual directional evolution (Metz *et al.*, 1992;

28 Dieckmann *et al.*, 1995; Dieckmann and Law, 1996; Geritz *et al.*, 2002).

1   When a mutant emerges, which occurs with probability μ per birth, we assume that its

2   phenotype $\mathbf{S}'$ follows a mutation probability distribution $M(\mathbf{S}' - \mathbf{S})$ given by a bivariate

3   normal distribution with mean $\mathbf{S}$ (Appendix A). The distribution of mutational step sizes

4   may depend on the direction of $\mathbf{S}' - \mathbf{S}$, according to the variance-covariance matrix of M.

5   In this trait space, evolutionary dynamics depend on the invasion-fitness function F and

6   the mutation probability distribution M. To describe this dependence, we consider a mono-

7   morphic population of phenotypes $\mathbf{S}_0$, and to simplify notation and analysis, we introduce a

8   locally normalized coordinate system $\mathbf{s} = (x, y)^{\mathrm{T}}$ having its origin at $\mathbf{S}_0$. This local coordi-

9   nate system is scaled so that the standard deviation of mutational step sizes, equaling the root-

10   mean-square mutational step size, is σ in all directions. The asymmetry (non-isotropy) of

11   mutations is thus absorbed into the invasion-fitness function, resulting in a normalized inva-

12   sion-fitness function denoted by $f(\mathbf{s}'; \mathbf{s})$.

13   The local shape of f around the origin $\mathbf{s} = 0$ ($\mathbf{S} = \mathbf{S}_0$) can be approximated by a Taylor

14   expansion in $\mathbf{s}$ and $\boldsymbol{\delta s} = (\delta x, \delta y)^{\mathrm{T}} = \mathbf{s}' - \mathbf{s}$ up to second order,

$$f(\mathbf{s}'; \mathbf{s}) = \mathbf{G}\ \boldsymbol{\delta s} + \frac{1}{2}\mathbf{s}^{\mathrm{T}}\mathbf{C}\ \boldsymbol{\delta s} + \frac{1}{2}\ \boldsymbol{\delta s}^{\mathrm{T}}\mathbf{D}\ \boldsymbol{\delta s}, \tag{1}$$

16   with the row vector $\mathbf{G} = (G_{\mathrm{x}}, G_{\mathrm{y}})$ and the matrices $\mathbf{C} = ((C_{\mathrm{xx}}, C_{\mathrm{xy}}), (C_{\mathrm{yx}}, C_{\mathrm{yy}}))^{\mathrm{T}}$ and

17   $\mathbf{D} = ((D_{\mathrm{xx}}, 0), (0, D_{\mathrm{yy}}))^{\mathrm{T}}$. The other possible terms in this expansion, proportional to $\mathbf{s}$ and

18   $\mathbf{s}^{\mathrm{T}}\mathbf{s}$, vanish because $f(\mathbf{s}; \mathbf{s}) = 0$ holds at population-dynamical equilibrium for arbitrary $\mathbf{s}$.

19   The vector $\mathbf{G} = \partial f(\mathbf{s}'; \mathbf{s}) / \partial \mathbf{s}'|_{\mathbf{s}'=\mathbf{s}=0}$ is the fitness gradient: it measures the steepest ascent of

20   f with respect to $\mathbf{s}'$, and thus describes directional selection for a population at the origin.

21   The matrix $\mathbf{C} = \partial^2 f(\mathbf{s}'; \mathbf{s}) / (\partial \mathbf{s}' \partial \mathbf{s})|_{\mathbf{s}'=\mathbf{s}=0}$ measures how directional selection changes as the

22   population deviates from the origin, and thus describes evolutionary convergence to, and/or

23   divergence from, the origin. The symmetric matrix $\mathbf{D} = \partial^2 f(\mathbf{s}'; \mathbf{s}) / \partial \mathbf{s}'^2|_{\mathbf{s}'=\mathbf{s}=0}$ measures the

24   second derivative, or curvature, of f with respect to $\mathbf{s}'$, and thus describes disruptive

25   and/or stabilizing selection at the origin. The local coordinate system $\mathbf{s} = (x, y)^{\mathrm{T}}$ can always

26   be chosen, by adjusting the directions of the x-and y-axes, so that $\mathbf{D}$ is diagonal and

27   $D_{\mathrm{xx}} \geq D_{\mathrm{yy}}$. Thus, when disruptive selection exists, it has maximum strength along the x-axis.

28   Notice that $\mathbf{G}$, $\mathbf{C}$, and $\mathbf{D}$ are functions of the base point $\mathbf{S}_0$.

Conditions for evolutionary-branching lines

1 **Conditions for evolutionary-branching lines**

2 A typical situation allowing evolutionary branching of a directionally evolving population

3 occurs when mutational step sizes are significantly smaller in one trait direction than in the

4 other, when considered in the original coordinate system $\mathbf{S} = (X, Y)^{\mathrm{T}}$. In this case, the popu-

5 lation quickly evolves in the direction of the larger step size until it no longer experiences

6 directional selection in that direction, while it continues slow directional evolution in the other

7 direction. Then, if the population experiences sufficiently strong disruptive selection along the

8 fast direction compared to directional selection along the slow direction, evolutionary branch-

9 ing may occur.

10 This conclusion has been demonstrated by Ito and Dieckmann (submitted), who analyti-

11 cally derived sufficient conditions for the existence of an evolutionary-branching line passing

12 through $\mathbf{S}_0$ (by focusing on trait-substitution sequences formed by invasions each of which

13 possesses maximum likelihood, so-called maximum-likelihood invasion paths or MLIPs). In

14 the locally normalized coordinate system $\mathbf{s} = (x, y)^{\mathrm{T}}$ at $\mathbf{S}_0$, these conditions come in three

15 parts,

16
$$G_x = 0,\tag{2a}$$

17
$$C_{xx} < 0,\tag{2b}$$

18 and

19
$$\frac{\sigma D_{xx}}{|G_y|} > \sqrt{2}.\tag{2c}$$

20 While Eqs. (2) were analytically derived assuming that C_{yy}, C_{xy}, C_{yx}, and D_{yy} are negli-

21 gible, it is expected that these conditions work well even when this simplifying assumption is

22 relaxed, as explained by Ito and Dieckmann (submitted). Eq. (2a) ensures the absence of di-

23 rectional selection in x. Eqs. (2a) and (2b) ensure convergence, through directional evolu-

24 tion, of monomorphic populations to the evolutionary-branching line $x = 0$. After sufficient

25 convergence, inequality (2c) ensures evolutionary branching, which according this is inequali-

26 ty occurs when disruptive selection D_{xx} orthogonal to $x = 0$ is sufficiently strong com-

1 pared to directional selection G_y along $x = 0$. The smaller the standard deviation σ of

2 mutation step sizes, the stronger disruptive selection D_{xx} must be relative to directional se-

3 lection G_y for evolutionary branching to occur.

4   Notice that as $\left| G_y \right| \to 0$, inequality (2c) converges to $D_{xx} > 0$, so that in this limiting case

5 conditions for evolutionary-branching lines in bivariate trait spaces become identical to condi-

6 tions for evolutionary-branching points in univariate trait spaces (Metz *et al.*, 1992; Geritz *et*

7 *al.*, 1997). Similarly, when $\sigma \to 0$, inequality (2c) requires $G_y = 0$ and $D_{xx} > 0$, which

8 shows that for infinitesimal mutation steps evolutionary branching can occur only in the ab-

9 sence of all directional selection.

10   By examining conditions (2) for all phenotypes $\mathbf{S}_0$ in a considered trait space, and by

11 then connecting those phenotypes that fulfill these conditions, evolutionary-branching lines

12 are identified. According to the derivation of conditions (2), it is ensured that any MLIP start-

13 ing from a monomorphic population of phenotypes sufficiently close to an evolutionary-

14 branching line immediately converges to that line and then brings about evolutionary branch-

15 ing (Ito and Dieckmann, submitted). Also trait-substitution sequences that are not MLIPs then

16 show a very high likelihood of evolutionary branching (Ito and Dieckmann, submitted).

17 **Conditions for evolutionary branching areas**

18 We now extend conditions for evolutionary-branching lines to evolutionary-branching areas.

19 As explained below, two special cases are analytically tractable; the extended conditions are

20 then obtained heuristically by treating intermediate cases through interpolation.

21   While conditions (2) were derived as sufficient conditions for evolutionary branching, it is

22 likely that in particular the equality condition (2a) is too strict, as evolutionary branching does

23 not require $G_x = 0$, but only that $\left| G_x \right|$ be sufficiently small. But how small is small enough?

24 To answer this question, we have to extend inequality (2c) to phenotypes that are not on an

25 evolutionary-branching line. For such phenotypes, the orthogonality between the directions of

26 directional selection and of maximum disruptive selection, which strictly holds on evolution-

27 ary-branching lines and is only negligibly disturbed in their immediate vicinity (Ito and

28 Dieckmann, submitted), is increasingly relaxed the farther these phenotypes are displaced

1   from such lines. Fortunately, the emergence of a protected dimorphism along MLIPs, which

2   underlies inequality (2c), can be studied analytically also for the opposite case, in which the

3   direction of directional selection is parallel to that of maximum disruptive selection (Appen-

4   dix B). By interpolating between these two special cases, we can generalize inequality (2c) to

5   intermediate cases, in which directional selection is neither orthogonal nor parallel to disrup-

6   tive selection,

7
$$\frac{\sigma D_{\mathrm{xx}}}{\left|\tilde{\mathbf{G}}\right|} > \sqrt{2} \ \text{ with } \ \tilde{\mathbf{G}} = (\sqrt{2}G_{\mathrm{x}}, G_{\mathrm{y}}). \tag{3a}$$

8   The factor $\sqrt{2}$ in the definition of $\tilde{\mathbf{G}}$ means that directional selection in x hinders evolu-

9   tionary branching in y slightly more, but this factor of $\sqrt{2}$, than directional selection in

10   y.

11   By combining inequalities (2b) and (3a), we obtain conditions for evolutionary-branching

12   areas, as it was Eq. (2a) that limits conditions (2) to being fulfilled just along lines. Evolution-

13   ary-branching areas always surround evolutionary-branching lines when such lines exist, but

14   additionally comprise phenotypes for which, in violation of Eq. (2a), directional evolution has

15   not yet converged to those lines.

16   Since the conditions for evolutionary-branching lines and areas are derived as sufficient

17   conditions (for the emergence of a protected dimorphism along MLIPs), the length of these

18   lines and the size of these areas are expected to be conservative. Thus, adjusting the threshold

19   value in Eq. (3a) may be useful for explaining observed patterns of evolutionary branching.

20   For this purpose, we introduce the parameter ρ with $0 < \rho \leq 1$ into Eq. (3a), which gives

21
$$\frac{\sigma D_{\mathrm{xx}}}{\left|\tilde{\mathbf{G}}\right|} > \sqrt{2}\rho. \tag{3b}$$

22   Below, we illustrate the effect of ρ by considering $\rho = 0.2$. We call the combination of

23   inequalities (2b) and (3b) the 20%-threshold condition for evolutionary-branching areas, and

24   we refer to areas fulfilling this condition as 20%-threshold areas. For specific procedures that

25   are useful for the practical identification of evolutionary-branching lines and areas, see Ap-

26   pendix C.

1   **Sizes and shapes of evolutionary-branching lines and areas**

2   As a simple example, we now briefly explain how an evolutionary-branching line and area are

3   identified around an evolutionary-branching point located at the origin of a trait space

4   $\mathbf{S} = (X, Y)^{\mathrm{T}}$. See Appendix E for details.

5   We assume that the strengths of convergence stability of the origin along the X- and Y-

6   axes are given by the two negative scalars C_{XX} and C_{YY}, respectively. We also assume that

7   the maximum disruptive selection in this original coordinate system occurs along the X-

8   axis, quantified by the positive scalar D_{XX} (i.e., $D_{\mathrm{XX}} > D_{\mathrm{YY}}$). In addition, we denote the

9   standard deviations of mutational step sizes along the X- and Y-axes by σ_{X} and σ_{Y},

10   respectively. We assume that these steps have no mutational correlation, $\sigma_{\mathrm{XY}} = 0$, and that

11   they are largest along the X-axis, $\sigma_{\mathrm{X}} > \sigma_{\mathrm{Y}}$. In this case, for each phenotype $\mathbf{S}_0 = (X_0, Y_0)^{\mathrm{T}}$

12   close to the origin, local normalization provides the matrices $\mathbf{G}$, $\mathbf{C}$, and $\mathbf{D}$ in Eq. (1),

13   without the need for any coordinate rotation; i.e., the x-axis is parallel to the X-axis.

14   By examining Eqs. (2) and Eq. (3a) based on the derived matrices $\mathbf{G}$, $\mathbf{C}$, and $\mathbf{D}$, we

15   find, expressed in the original coordinate system, an evolutionary-branching line as a straight

16   line segment,

17
$$X_0 = 0 \quad \text{and} \quad |Y_0| \; r_{\mathrm{Y}}, \tag{4}$$

18   and an evolutionary-branching area as a filled ellipse,

19
$$\frac{X_0^2}{r_{\mathrm{X}}^2} + \frac{Y_0^2}{r_{\mathrm{Y}}^2} < 1, \tag{5a}$$

20   with a radius of

21
$$r_{\mathrm{X}} = \frac{\sigma_{\mathrm{X}} D_{\mathrm{XX}}}{2|C_{\mathrm{XX}}|} \tag{5b}$$

22   along the X-axis and a radius of

23
$$r_{\mathrm{Y}} = \frac{\sigma_{\mathrm{X}} D_{\mathrm{XX}}}{\sqrt{2}|C_{\mathrm{YY}}|} \cdot \frac{\sigma_{\mathrm{X}}}{\sigma_{\mathrm{Y}}} \tag{5c}$$

24   along the Y-axis.

1   Notice that the length of the evolutionary-branching line coincides with the radius of the

2   evolutionary-branching area along the Y-axis. According to Eqs. (5), if the difference in

3   magnitude between σ_{X} and σ_{Y} is kept small, large mutational step sizes and/or strong dis-

4   ruptive selection pressures result in large evolutionary-branching areas. On the other hand,

5   according to Eq. (5c), when σ_{Y} is small compared to σ_{X}, the shape of the evolutionary-

6   branching area is elongated along the Y-axis, even if σ_{X} is small. Since infinitesimally

7   small σ_{Y} make this situation identical to that of a univariate trait space comprising trait X

8   alone, Eq. (5b) may work also for predicting one-dimensional evolutionary-branching areas

9   surrounding evolutionary-branching points in univariate trait spaces.

FIRST EXAMPLE: RESOURCE-COMPETITION MODEL WITH

EVOLVING NICHE POSITIONS

12   In this section, we apply our conditions for evolutionary-branching lines and areas to a model

13   of niche evolution under intraspecific resource competition (Vukics and Meszéna, 2003; Ito

14   and Dieckmann, 2007), which is a bivariate extension of seminal models by MacArthur and

15   Levins (MacArthur and Levins, 1967; MacArthur, 1972) and Roughgarden (1974, 1976). This

16   example illustrates how an evolutionary-branching point transforms into an evolutionary-

17   branching line when differences in mutational step sizes among two trait directions become

18   sufficiently large.

Model description

20   We consider a bivariate trait space $\mathbf{S} = (X, Y)^{\mathrm{T}}$, with X and Y denoting evolving traits

21   that determine a phenotype's bivariate niche position. The growth rate of phenotype $\mathbf{S}_i$ is

22   given by

$$\frac{\mathrm{d}n_i}{\mathrm{d}t} = n_i[1 - \sum_{j=1}^{L} \alpha(\mathbf{S}_i - \mathbf{S}_j)n_j / K(\mathbf{S}_i)], \tag{6a}$$

24   where L is the number of resident phenotypes. The carrying capacity $K(\mathbf{S}_i)$ of phenotype

25   $\mathbf{S}_i$ is given by an isotropic bivariate normal distribution,

$$K(\mathbf{S}_i) = K_0 \exp(-\tfrac{1}{2}|\mathbf{S}_i|^2 / \sigma_{\mathrm{K}}^2), \tag{6b}$$

1   with maximum K_0, mean $(0,0)^\mathrm{T}$, and standard deviation σ_K. The strength $\alpha(\mathbf{S}_i - \mathbf{S}_j)$ of

2   competition between phenotype $\mathbf{S}_i$ and phenotype $\mathbf{S}_j$ is also given by an isotropic bivari-

3   ate normal distribution,

$$\alpha(\mathbf{S}_i - \mathbf{S}_j) = \exp(-\tfrac{1}{2}\left|\mathbf{S}_i - \mathbf{S}_j\right|^2 / \sigma_\alpha^2), \qquad (6c)$$

5   with maximum 1, mean $(0,0)^\mathrm{T}$, and standard deviation σ_α, so the strength of competition is

6   maximal between identical phenotypes $\mathbf{S}_i = \mathbf{S}_j$ and monotonically declines with phenotypic

7   distance $\left|\mathbf{S}_i - \mathbf{S}_j\right|$.

8   In this model, carrying capacity is maximal at the origin $\mathbf{S} = (0,0)^\mathrm{T}$, which therefore

9   serves as a unique convergence stable phenotype, or global evolutionary attractor, to which

10 monomorphic populations converge through directional evolution. After sufficient conver-

11 gence, if the width σ_α of the competition kernel is narrower than the width σ_K of the car-

12 rying-capacity distribution, the resultant fitness landscape has a minimum at the origin, which

13 induces evolutionary branching of the evolving population. Thus, $\sigma_\alpha < \sigma_\mathrm{K}$ is the condition

14 for existence of an evolutionary-branching point in this model (Vukics and Meszéna, 2003),

15 in analogy with the univariate case (Roughgarden, 1972; Dieckmann and Doebeli, 1999).

16   As for the mutation probability distribution, we define its variance-covariance matrix so

17 that the standard deviation of mutational step sizes has a maximum σ_1 in the direction of

18 $\mathbf{e}_1 = (-1,1)^\mathrm{T}$ and a minimum σ_2 in the direction of $\mathbf{e}_2 = (1,1)^\mathrm{T}$.

19   Notice that fitness in this model is rotationally symmetric in terms of the traits X and

20 Y (i.e., rotating all phenotypes around the origin does not change their fitnesses). Thus, a

21 sensitivity difference of the normalized invasion-fitness function can arise only from the con-

22 sidered difference in mutational step sizes along the two directions $\mathbf{e}_1$ and $\mathbf{e}_2$.

Predicted evolutionary-branching lines and areas

24 When mutational step sizes are isotropic, the predicted evolutionary-branching area forms a

25 circle around the evolutionary-branching point, and contains no evolutionary-branching line

26 (not shown). In this case, occurrences of evolutionary branching are explained well by the

27 evolutionary-branching point alone. Because of the rotational symmetry in fitness, there is no

1   restriction on the direction of evolutionary branching, so that evolutionary diversification can

2   occur in any direction (Vukis and Meszéna, 2003). Although this case is reminiscent of that of

3   a univariate trait defined by the distance from the evolutionary-branching point, these two

4   cases are not equivalent: this is because in the univariate case disruptive selection and direc-

5   tional selection are always parallel, while in the isotropic bivariate case disruptive selection

6   may be orthogonal to directional selection.

7   Figure 2a shows that when the difference in mutational step size between directions $\mathbf{e}_1$

8   and $\mathbf{e}_2$ is substantial (e.g., $\sigma_1 / \sigma_2 = 3$), the evolutionary-branching line and area expand in

9   the direction of the smaller mutational step size ($\mathbf{e}_2$ in this case). In addition, the direction of

10   expected evolutionary diversification is getting the more restricted to $\mathbf{e}_1$ the larger this dif-

11   ference becomes. [If $\mathbf{e}_1$ and $\mathbf{e}_2$ were pointing along the Y- and X-axes, respectively, the

12   situation would correspond to Eqs. (4) and (5).] In Fig. 2a, the short purple line and the small

13   purple area (both situated within the light-purple area) depict the predicted evolutionary-

14   branching line and area, with their colors indicating the predicted direction of diversification.

15   Because of the difference in mutational step sizes between the two directions, it is expected

16   that a monomorphic population quickly converges to the line $Y = X$ (gray arrows) and then

17   slowly converges to the evolutionary-branching area. Evolutionary branching is expected to

18   occur at the latest once evolution has reached this area, because our conditions for an evolu-

19   tionary-branching area are derived as sufficient conditions and imply the possibility of an

20   immediate start of evolutionary branching of a monomorphic population in its inside. Accord-

21   ingly, evolutionary branching may occur well before the population has reached the evolu-

22   tionary-branching area. The light-purple area shows the corresponding 20%-threshold area,

23   comprising all phenotypes that fulfill the 20%-threshold condition for evolutionary-branching

24   areas. By definition, an evolutionary-branching area is always included in the corresponding

25   20%-threshold area. The larger the difference in mutational step sizes between the two direc-

26   tions, the longer the evolutionary-branching line and the more elongated the evolutionary-

27   branching area, as predicted by Eq. (5c)

1 **Comparison with actual evolutionary dynamics**

2 Figure 2b shows occurrences of evolutionary branching in numerically calculated evolution-

3 ary dynamics starting from monomorphic populations with phenotypes randomly chosen

4 across the shown trait space: each occurrence is depicted by an open triangle whose color in-

5 dicates the direction of that particular evolutionary branching. The evolutionary dynamics are

6 numerically calculated as trait-substitution sequences according to the oligomorphic stochas-

7 tic model of adaptive dynamics theory (Ito and Dieckmann, 2007; for the sake of computa-

8 tional efficiency, phenotypes with densities below a threshold ε_e are removed, with the val-

9 ue of ε_e being immaterial as long as it is small enough). The relative shape of the cluster of

10 occurrences is characterized well by the evolutionary-branching area, or here almost equiva-

11 lently, by the evolutionary-branching line. Moreover, the absolute shape, and hence the size,

12 of this cluster is well matched by that of the 20%-threshold area. The fact that the colors of

13 the triangles in Fig. 2b are very similar to that of the evolutionary-branching area in Fig. 2a

14 demonstrates that also the predicted and actual directions of diversification are in good

15 agreement.

16 Figure 2b shows two evolutionary trajectories, depicted as dark-yellow and green curves,

17 respectively. These illustrate that monomorphic populations initially converge to the line

18 $Y = X$. Then, if the population is already inside the evolutionary-branching area, it immedi-

19 ately undergoes evolutionary branching, as expected (green curves in Fig. 2b and Fig. 2d). In

20 contrast, if the population still remains outside the evolutionary-branching area, it continues

21 directional evolution along the line $Y = X$ towards the evolutionary-branching area. As ex-

22 pected, evolutionary branching may occur before the population has reached the evolutionary-

23 branching area (dark-yellow curves in Fig. 2b and Fig. 2c).

24 In summary, this first example shows how differences in mutational step sizes among trait

25 directions can transform an evolutionary-branching point into an evolutionary-branching line

26 or an elongated evolutionary-branching area.

SECOND EXAMPLE: RESOURCE-COMPETITION MODEL WITH EVOLVING NICHE POSITION AND NICHE WIDTH

In this section, based on another type of resource-competition model, we show that an evolutionary-branching area can exist without containing any evolutionary-branching point.

Model description

For phenotypes $\mathbf{S} = (X, Y)^{\mathrm{T}}$ in our second example, the trait X still determines the phenotype's niche position, like in the first model, whereas the trait Y now determines the phenotype's niche width, differently from the first model. This niche width can be interpreted in terms of the variety of resource types utilized by the phenotype. We assume a constant and unimodal distribution $R(z)$ of univariate resource types z, given by a normal distribution,

$$R(z) = R_0 \mathrm{N}(z, m_{\mathrm{R}}, \sigma_{\mathrm{R}}^2),\tag{7a}$$

with $\mathrm{N}(z, m, \sigma^2) = \exp(-\tfrac{1}{2}(z - m)^2 / \sigma^2) / (\sqrt{2\pi}\sigma)$. Here, R_0, m_{R}, and σ_{R} denote the resource distribution's integral, mean, and standard deviation. Similarly, the niche of a phenotype $\mathbf{S}_i$ is specified by a normal distribution across resource types z, with mean X_i (niche position) and standard deviation Y_i (niche width),

$$c(z, \mathbf{S}_i) = \mathrm{N}(z, X_i, Y_i^2).\tag{7b}$$

The rate of potential resource gain of phenotype $\mathbf{S}_i$ per unit of its biomass is given by the overlap integral, over all resource types z, of its niche $c(z, \mathbf{S}_i)$ and the resource distribution $R(z)$. The corresponding rate of actual resource gain $g(\mathbf{S}_i)$ incorporates a functional response, derived in Appendix D as an extension of the Beddington-DeAngelis-type functional response (Beddington, 1975; DeAngelis *et al.*, 1975), known to ensure both saturation of consumption and interference competition among consumers. On this basis, the growth rate of phenotype $\mathbf{S}_i$ is given by

$$\frac{\mathrm{d}n_i}{\mathrm{d}t} = n_i[\lambda g(\mathbf{S}_i) - d(Y_i)],\tag{7c}$$

1   where the constant λ measures trophic efficiency (i.e., biomass production per biomass

2   gain) and $d(Y_i)$ is the biomass loss of phenotype $\mathbf{S}_i$ due to basic metabolism and natural

3   death, with the dependence on Y_i reflecting costs of specialization or generalization.

4   As for the mutation distribution, we use a simple bivariate normal distribution in which

5   the standard deviation of mutational step sizes has its maximum σ_X in the X-direction and

6   its minimum σ_Y in the Y-direction. See Appendix E for further model details.

Predicted evolutionary-branching lines and areas

8   Figure 3a shows the directional evolution (gray arrows) of monomorphic populations and the

9   predicted evolutionary-branching lines and areas, as in Fig. 2a, for the case that specialization

10   (narrow niche width) is costly. This shows that niche position and niche width directionally

11   evolve so as to become more similar, respectively, to the center and width of the resource

12   distribution. We find two kinds of evolutionary-branching areas. As indicated by the color

13   coding, the small blue evolutionary-branching area around the center of the shown trait space

14   induces evolutionary branching in the direction of niche width. This evolutionary-branching

15   area contains an evolutionary-branching point at its center and is attracting any monomorphic

16   population in the trait space. In this regard, this evolutionary-branching area is similar to that

17   in the first model. In contrast, the red evolutionary-branching area around the bottom of the

18   shown trait space contains no evolutionary-branching point, although it does contain an evo-

19   lutionary-branching line along $X = 0.5$. Moreover, as indicated by the color coding, this evo-

20   lutionary-branching line and area induce evolutionary-branching in the direction of niche po-

21   sition. It is therefore clear that the two identified evolutionary-branching areas are qualitative-

22   ly different from each other.

Comparison with actual evolutionary dynamics

24   Figure 3b shows occurrences of evolutionary branching in numerically calculated evolution-

25   ary dynamics, as in Fig. 2b. There exist three clusters: a blue one around the center, a small

26   red one around $\mathbf{S} = (0.5, 0.16)^{\mathrm{T}}$, and a large red one along the bottom of the shown trait

27   space. Except for the small red cluster, the shapes of these clusters coincide well with the two

identified evolutionary-branching areas. Also, as shown by the color coding, the directions of observed diversifications are predicted well by those areas.

As for the blue evolutionary-branching area, the observed process of evolutionary branching in niche width (dark-yellow curves in Fig. 3b) is always slow, as shown in Fig. 3c. In contrast, the large red evolutionary-branching area induces fast and repeated evolutionary branching in niche position (green curves in Fig. 3b), generating four lineages at the end of the time window in Fig. 3d. The timescale difference between these two types of branching dynamics exceeds a factor of 100.

This difference in evolutionary speed can be explained as follows. When a population comes close to the blue evolutionary-branching area, the shape of its niche is similar to the resource distribution, resulting in weak selection pressures, including disruptive selection. In this case, the process of evolutionary branching is therefore expected to be slow. On the other hand, when a population is close to, or located inside, the red evolutionary-branching area, its niche is much narrower than the resource distribution. This situation creates strong disruptive selection in niche position. In this case, the process of evolutionary branching is thus expected to proceed rapidly.

This second example shows that our conditions for evolutionary-branching areas can identify such areas containing no evolutionary-branching point. Here, such an area induces a qualitatively different mode of evolutionary branching than the also existing evolutionary-branching area that contains an evolutionary-branching point. Notice, however, that our conditions for evolutionary-branching areas do not explain the separation between the small and large red clusters in Fig. 3b. In addition, the size of the blue cluster in Fig. 3b is much larger than that of the corresponding 20%-threshold area in Fig. 3a, which is not explained either.

THIRD EXAMPLE: PREDATOR-PREY MODEL WITH EVOLVING NICHE POSITIONS

In this section, based on a predator-prey model, we show that evolutionary branching can occur even if a model's entire trait space contains no evolutionary-branching point, so that any occurrence of evolutionary branching is explained by evolutionary-branching lines and areas.

1   Model description

2   The third model is a modification of the second model towards predator-prey interactions.

3   This model was developed by Ito *et al.* (2009); see Appendix F for details. As in the first and

4   second models, trait X still determines a phenotype's niche position. Now, however, trait

5   Y is not a niche width as in the second model, but describes the niche position at which the

6   corresponding phenotype can be consumed as a resource, and is therefore potentially preyed

7   upon by other phenotypes. We thus refer to X and Y as predator-niche position and prey-

8   niche position, respectively. Accordingly, phenotype $\mathbf{S}_i$ exists not only as a consumer (pred-

9   ator) with niche

$$c(z,\mathbf{S}_i) = \mathrm{N}(z, X_i, \sigma_c^2), \tag{8a}$$

11   but also provides a resource (prey) distribution for predators, with each of its biomass units

12   contributing according to

$$r(z,\mathbf{S}_i) = \mathrm{N}(z, Y_i, \sigma_r^2), \tag{8b}$$

14   where the widths of these two distributions are constant and given by σ_c and σ_r, respec-

15   tively. The basal-resource distribution $B(z) = R_0 \mathrm{N}(z, m_R, \sigma_R^2)$, with integral R_0, mean m_R,

16   and standard deviation σ_R, is analogous to the resource distribution in Eq. (7a) for the se-

17   cond model. In analogy with the second model, the rates of resource gain and biomass loss of

18   phenotype $\mathbf{S}_i$, denoted by $g(\mathbf{S}_i)$ and $l(\mathbf{S}_i)$, respectively, are obtained as overlap integrals

19   of niches and existing resources. Consequently, the growth rate of phenotype $\mathbf{S}_i$ is given by

$$\frac{\mathrm{d}n_i}{\mathrm{d}t} = n_i[\lambda g(\mathbf{S}_i) - l(\mathbf{S}_i) - d], \tag{8c}$$

21   where the rate d of biomass loss by metabolism and natural death is now assumed to be

22   constant, differently from the second model.

23   As in the second model, we use a simple bivariate normal mutation distribution in which

24   the standard deviation of mutational step sizes has its maximum σ_X in the X-direction and

25   its minimum σ_Y in the Y-direction.

1 Predicted evolutionary-branching lines and areas

2 Figure 4a shows the directional evolution (gray arrows) and predicted evolutionary-branching

3 lines and areas, as in Fig. 2a and Fig. 3a. This shows that monomorphic populations direc-

4 tionally evolve so that their prey-niche positions become more distant from their predator-

5 niche positions, while their predator-niche positions become closer to their prey-niche posi-

6 tion and/or the mean of the basal-resource distribution (Ito *et al.*, 2009).

7 A unique evolutionarily singular point at $\mathbf{S} = (0.5, 0.5)^{\mathrm{T}}$ matches the center of the basal-

8 resource distribution at $z = m_{\mathrm{R}} = 0.5$. This corresponds to a cannibalistic population exploit-

9 ing both the basal resource and itself. As the basal-resource distribution is assumed to be wid-

10 er than the predator niche, $\sigma_{\mathrm{R}} > \sigma_{\mathrm{c}}$, disruptive selection along X is expected, similarly to

11 the first example. However, the zero-isocline of the fitness gradient in the Y-direction (thick

12 grey curve in Fig. 4a) repels monomorphic populations in the Y-direction, although the cor-

13 responding zero-isocline in the X-direction (thin black curve) attracts them in the X-

14 direction. Therefore, depending on the relative mutation probabilities and mutational step siz-

15 es in X and Y, the evolutionarily singular point at the intersection of those two zero-

16 isoclines may not be convergence stable (Dieckmann and Law, 1996; Leimar, 2009; for anal-

17 ogous results for multilocus genetics, see Mattessi and Di Pasquale, 1996), in which case

18 there is no evolutionary-branching point in this trait space.

19 According to our conditions for evolutionary-branching lines, evolutionary branching by

20 disruptive selection in X may occur when a phenotype's prey-niche position becomes suffi-

21 ciently distant from its predator-niche position, so that directional selection on the prey-niche

22 position becomes sufficiently weak. As thus expected, there exist evolutionary-branching

23 lines along the evolutionary zero-isocline for X (red line segments). Evolutionary-

24 branching areas also exist, but are very thin; only the 20%-threshold areas are sufficiently

25 large to become visible in Fig. 4a (light-red areas). As shown by the color coding for evolu-

26 tionary-branching lines and areas, evolutionary branching is solely expected in the direction

27 of predator-niche position.

There also exists a very small evolutionary-branching area around the evolutionarily sin-
gular point at the center, which, however, may induce evolutionary branching only when the
initial phenotype is located within this area, as this singular point is lacking convergence sta-
bility.

Comparison with actual evolutionary dynamics

Figure 4b shows occurrences of evolutionary branching in numerically calculated evolution-
ary dynamics, as in Fig. 2b and Fig. 3b. The shapes of the clusters, as well as the directions of
observed evolutionary branching, are predicted well by the evolutionary-branching lines and
areas. Also the sizes of these clusters are predicted well by the 20%-threshold areas.

As shown in Fig. 4b (green curves) and Fig. 4d, a monomorphic population first converg-
es to the evolutionary zero-isocline for X (thin black curve), and then brings about evolu-
tionary branching when it has come sufficiently close to one of the evolutionary-branching
lines.

Also, as predicted, evolutionary branching in the small evolutionary-branching area at the
center is possible, provided the initial phenotype is located within this area (dark-yellow
curves in Fig. 4b and Fig. 4c). However, since this evolutionary-branching area is very small
and does not contain an evolutionary attractor, almost all observed diversifications are in-
duced by the identified evolutionary-branching lines.

Even when the predator niche is wider than the prey niche and the basal-resource distribu-
tion ($\sigma_c > \sigma_r, \sigma_R$; e.g., when $\sigma_c = 0.081$ slightly exceeds $\sigma_r = \sigma_R = 0.08$, while
$\sigma_X = 0.003$ and $\sigma_X = 0.0003$), evolutionary-branching lines can exist and induce diversifi-
cation (not shown). In any case, the initial evolutionary branching always occurs adjacent to
the evolutionary-branching lines.

Interestingly, evolutionary branching in this model can be recurrent: this may result in
complex food webs of coexisting phenotypes, including the evolutionarily stable emergence
of multiple trophic levels (Ito *et al.*, 2009).

DISCUSSION

In this study we have presented conditions for evolutionary-branching lines and areas, and have explored their utility by numerically analyzing evolutionary branching in three different eco-evolutionary models defined with bivariate trait spaces. The first model, a resource-competition model with evolving niche positions, has shown how an evolutionary-branching point transforms into an evolutionary-branching line and elongated evolutionary-branching area, due to differences in mutational step sizes among the two trait directions. The second model, a resource-competition model with evolving niche position and niche width, has shown the existence of an evolutionary-branching line and area containing no evolutionary-branching point, which induce a qualitatively different mode of evolutionary branching than the also existing evolutionary-branching point. The third model, a predator-prey model with evolving predator- and prey-niche positions, has shown that even when a model's entire trait space contains no evolutionary-branching point, evolutionary branching may still be bound to occur along evolutionary-branching lines and within evolutionary-branching areas. Below we discuss these phenomena in greater detail.

To understand the transformation of an evolutionary-branching point into an evolutionary-branching line and an elongated evolutionary-branching area in the first model, it is helpful to recognize that an evolutionary-branching line becomes straight and infinitely long in the limit of mutational step sizes parallel to that line converging to 0. In this limit, the resultant evolutionary dynamics are effectively univariate and occur vertically to the evolutionary-branching line. In the resultant effectively univariate trait space, the evolutionary-branching line then corresponds to an evolutionary-branching point. Thus, the curvatures and finite lengths of evolutionary-branching lines can be appreciated as resulting from eco-evolutionary settings that are intermediate between the two extremes of effectively univariate trait spaces (Metz *et al.*, 1992; Geritz *et al.*, 1997) and fully bivariate ones (Ackermann and Doebeli, 2004; Egas *et al.*, 2005; Vukics and Meszéna, 2003; Ito and Dieckmann, 2007).

In our examples, such settings are created by considering different mutational step sizes in two directions of trait space. Importantly, the very same effects also arise when invasion-

fitness functions possess different sensitivities to trait changes in two directions of trait space. This is simply because such sensitivity differences can be translated into differences in mutational step sizes by suitably rescaling trait space. In many settings, these two types of differences are formally indistinguishable, and are jointly captured by the local normalization of trait space we have described. The situation is different when the traits contributing to a multivariate phenotype happen to be defined on the same, or naturally comparable, scales. In such special settings, it is feasible to assess whether the emergence of evolutionary-branching lines and areas is due to differences in mutational steps, differences in fitness sensitivities, or a combination thereof.

The existence of evolutionary-branching lines and areas containing no evolutionary-branching points, observed in our second and third examples, will go unnoticed by any analysis restricted to identifying evolutionary-branching points. Extending past and future theoretical studies by accounting for our conditions for evolutionary-branching lines and areas is therefore advisable, as modes of evolutionary diversification in the underlying models may otherwise be missed.

For instance, our conditions have revealed that if disruptive selection is particularly strong, evolutionary branching can occur even in the face of considerable directional selection. This mode is characterized by a rapid progression of the diversification, as illustrated by our second example when a population's niche is much narrower than the resource distribution. In this situation, evolutionary branching in niche position is rapidly repeated, accompanied by gradual evolutionary generalization. Consequently, such evolutionary dynamics are expected to occur also in models examined in previous studies of the joint evolution of niche position and niche width (Ackerman and Doebeli, 2003; Egas and Dieckmann, 2004; Ito and Shimada, 2007). Accordingly, this finding could open up new perspectives for understanding empirically observed instances of adaptive radiation, such as in Darwin's finches (Grant and Grant, 2008), cichlid fish (Seehausen, 2006), sticklebacks (Bell and Foster, 1994; Schluter, 2000), and anolis lizards (Losos, 2009).

Our third model, a predator-prey model with evolving niche positions, illustrates how it is straightforward to draw qualitative conclusions from our conditions for evolutionary-

1   branching lines and areas. Specifically, when the width of the predator niche is similar to that

2   of the basal-resource distribution, there can be no particularly strong disruptive selection.

3   Therefore, directional selection vertical to the disruptive selection needs to be sufficiently

4   weak if evolutionary branching is to occur. This is possible only when a phenotype's prey-

5   niche position is distant from its predator-niche position, giving rise to the evolutionary-

6   branching lines and areas shown in Fig. 4a. Applying our conditions, analogous evolutionary-

7   branching lines and areas can be identified also in other predator-prey models (Ito and

8   Ikegami, 2006; Ito *et al.*, 2009) that are comparable to our third model (not shown).

9   In a similar vein, we can consider predator-prey models that differ from our third model.

10 For example, in the predator-prey model by Brännström *et al.* (2010), the predator-niche and

11 prey-niche positions are given by a single trait, resulting in a univariate trait space that has a

12 single evolutionary-branching point. While univariate trait spaces naturally cannot contain

13 evolutionary-branching lines or areas, our findings here suggest that it will be interesting to

14 extend the model by Brännström *et al.* (2010) so that the predator-niche and prey-niche posi-

15 tions can evolve separately: the previously found evolutionary-branching point is then ex-

16 pected to transform into evolutionary-branching lines and areas, and additional evolutionary-

17 branching lines and areas containing no evolutionary-branching point might emerge.

18   It may also be worthwhile to revisit, in light of our conditions, a study by Doebeli and

19 Dieckmann (2000) that also demonstrated evolutionary branching driven by predator-prey

20 interactions. Their model considered two univariate traits, one for a predator's predator-niche

21 position and one for a prey's prey-niche position: thus, the predator can adapt only in terms of

22 its predator-niche position, while the prey can adapt only in terms of its prey-niche position.

23 Although this doubly univariate setting formally differs from the bivariate setting we have

24 analyzed in the present study, applying our conditions might help reveal the existence of evo-

25 lutionary-branching lines and areas in the model by Doebeli and Dieckmann (2000).

26   Our conditions for evolutionary-branching lines and areas are analytically derived from

27 assessing the potential for immediate evolutionary branching of a monomorphic population

28 (Ito and Dieckmann, submitted). Since these conditions are sufficient, but not necessary, evo-

29 lutionary branching in numerically calculated evolutionary dynamics may occur under a wid-

er range of conditions, reflecting the gradual integration of local probabilistic rates of evolutionary branching along monomorphic evolutionary trajectories. Accordingly, no full agreement between these two perspectives can be expected. It is therefore encouraging that the results presented here have demonstrated that the positions and shapes of clusters of occurrences of evolutionary branching are well predicted by evolutionary-branching areas. Moreover, the sizes of those clusters are well predicted by the corresponding 20%-threshold areas in many, but not all, cases (see, e.g., the small blue evolutionary-branching area in Fig. 3a). A further potential cause of disparity is that our conditions for evolutionary-branching areas use only partial information about the local selection pressures, assuming that the second-order derivatives C_{yy}, C_{xy}, C_{yx}, and D_{yy} (as measured in the locally normalized coordinate systems) are not important. Occasionally, these additional characteristics of the local shapes of fitness landscapes might well affect the local probabilistic rates of evolutionary branching. A formal analysis of these effects, if it turned out to be technically feasible, might improve predictive performance.

Our results in this study are based on restrictive assumptions, such as small mutation rates, large population sizes, bivariate normal mutation distributions, and asexual reproduction. It will therefore be desirable to examine the robustness of our results by relaxing or varying those assumptions. First, when mutation rate is large, evolutionary dynamics are no longer described by trait-substitution sequences, but instead amount to gradual changes of polymorphic trait distributions. In this case, one could attempt to define an effective mutation probability distribution by considering the convolution of the phenotype distribution with the actual mutation probability distribution. As this convolution is always wider than the actual mutation probability distribution alone, and as the conditions for evolutionary-branching lines and areas predict higher likelihoods of evolutionary branching for larger mutational step sizes, large mutation rates may effectively increase those likelihoods. Second, when population sizes are not sufficiently large, demographic stochasticity may destroy protected dimorphisms shortly after their emergence, as the two coexisting phenotypes initially are almost ecologically neutral (Claessen *et al.*, 2007, 2008). This can suppress evolutionary branching. Third, variations of the mutation probability distribution, keeping its variance-covariance matrix constant, may

1 enhance or suppress the likelihood of evolutionary branching, depending on the specific

2 shapes considered. Fourth, sexual reproduction is expected to suppress evolutionary branch-

3 ing, as the continuous production of intermediate offspring phenotypes counteracts diversifi-

4 cation by disruptive selection (Dieckmann and Doebeli, 1999; Kisdi *et al*., 1999).

5   As for mutation rates and mutation probability distributions, Ito and Dieckmann (submit-

6 ted) have already shown that (for $C_{yy}, C_{xy}, C_{yx}, D_{yy} = 0$ in the normalized coordinate sys-

7 tems) the derived conditions for evolutionary-branching lines are reasonably robust to making

8 mutation rates larger and letting mutation distributions deviate from being normal. This ro-

9 bustness may nevertheless be affected by making population sizes smaller than those already

10 analyzed, so that demographic stochasticity becomes relatively more important. As for sexual

11 reproduction, evolutionary branching of sexual populations induced by evolutionary-

12 branching lines has been demonstrated numerically by Dieckmann and Ito (2007). This pre-

13 ceding work considered the joint evolution of several quantitative traits, an ecological trait

14 and mating traits, with additive multilocus genetics, free recombination, and not-small muta-

15 tion rates. This analysis has demonstrated that when the evolution of assortative mating is

16 difficult, evolutionary branching will often be suppressed, which implies that sexual repro-

17 duction may cause likelihoods of evolutionary branching to be overestimated by the condi-

18 tions reported here for evolutionary-branching lines and areas in asexual populations.

19   Although we have focused on bivariate trait spaces in this study (to facilitate visual in-

20 spection), the conditions for evolutionary-branching lines derived by Ito and Dieckmann

21 (submitted) readily apply to multivariate trait spaces, and our conditions for evolutionary-

22 branching areas generalize analogously. Moreover, our conditions for evolutionary-branching

23 lines and areas are expected to be applicable also to coevolutionary dynamics and to the dy-

24 namics of subsequent evolutionary branching after a primary evolutionary branching has oc-

25 curred. From a computational perspective, it is promising to interleave the application of our

26 conditions with the time integration of the canonical equation of adaptive dynamics theory

27 (Dieckmann and Law, 1996): in this way, the deterministic approximation of evolutionary

28 branching provided by our conditions can be integrated with the deterministic approximation

1 of directional evolutionary and coevolutionary dynamics provided by the canonical equation,

2 resulting in a deterministic oligomorphic model of phenotypic evolution.

3   In conclusion, our conditions for evolutionary-branching lines and areas have yielded two

4 new insights into evotionary branching. First, evolutionary-branching points can transform

5 into evolutionary-branching lines and areas, due to differences in mutational steps and/or fit-

6 ness sensitivities among directions in trait spaces. Second, evolutionary-branching lines and

7 areas can exist independently of evolutionary-branching points, which allows diversification

8 even when an entire trait space contains not a single evolutionary-branching point.

REFERENCES

20 Ackermann, M. and Doebeli, M. 2004. Evolution of niche width and adaptive diversification.

21   *Evolution*, **58**: 2599-2612.

22 Beddington, J.R. 1975. Mutual interference between parasites or predators and its effect on

23   searching efficiency. *J. Anim. Ecol.*, **44**: 331-340.

24 Bell, M.A. and Foster, S.A. 1994. The Evolutionary Biology of the Threespine Stickleback.

25   Oxford University Press, Oxford.

26 Brännström, Å., Loeuille, N., Loreau, M. and Dieckmann, U. 2011. Emergence and mainte-

27   nance of biodiversity in an evolutionary food-web model. *Theor. Ecol.*, **4**: 467-478.

1   Claessen, D., Andersson, J., Persson, L., and de Roos, A.M. 2007. Delayed evolutionary
2   branching in small populations. *Evol. Ecol. Res.*, **9**: 51-69.

3   Claessen, D., Andersson, J. and Persson, L. 2008. The effect of population size and recombi-
4   nation on delayed evolution of polymorphism and speciation in sexual populations. *Am.*
5   *Nat.*, **172**: E18-E34.

6   DeAngelis, D.L., Goldstein, R.A. and O'Neill, R.V. 1975. A model for tropic interaction.
7   *Ecology*, **56**: 881-892.

8   Dieckmann, U., Brännström, Å., HilleRisLambers, R. and Ito, H.C. 2007. The adaptive dy-
9   namics of community structure. In: *Mathematics for Ecology and Environmental Scienc-*
10   *es*, eds. Takeuchi Y, Sato K and Iwasa Y, pp. 145-177. Springer Verlag, Berlin.

11 Dieckmann, U. and Doebeli, M. 1999. On the origin of species by sympatric speciation. *Na-*
12   *ture*, **400**: 354-357.

13 Dieckmann, U., Doebeli, M., Metz, J.A.J. and Tautz, D. eds. 2004. Adaptive Speciation.
14   Cambridge University Press, Cambridge.

15 Dieckmann, U., Marrow, P. and Law, R. 1995. Evolutionary cycling in predator-prey interac-
16   tions: population dynamics and the Red Queen. *J. Theor. Biol.*, **176**: 91-102.

17 Dieckmann, U. and Law, R. 1996. The dynamical theory of coevolution: a derivation from
18   stochastic ecological processes. *J. Math. Biol.*, **34**: 579-612.

19 Dieckmann, U., Metz, J.A.J., Doebeli, M. and Tautz, D. 2004. Adaptive Speciation. Cam-
20   bridge University Press, Cambridge.

21 Doebeli, M. 1996. A quantitative genetic model for sympatric speciation. *J. Evol. Biol.*, **9**:
22   893-909.

23 Doebeli, M. and Dieckmann, U. 2000. Evolutionary branching and sympatric speciation
24   caused by different types of ecological interactions. *Am. Nat.*, **156**: S77-S101.

25 Doebeli, M. and Dieckmann, U. 2003. Speciation along environmental gradients. *Nature*, **421**:
26   259-264.

27 Durinx, M. and Van Dooren, T.J. 2009. Assortative mate choice and dominance modification:
28   alternative ways of removing heterozygote disadvantage. *Evolution*, **63**: 334-352.

1 Egas, M., Sabelis, M.W. and Dieckmann, U. 2005. Evolution of specialization and ecological
2   character displacement of herbivores along a gradient of plant quality. *Evolution*, **59**: 507-
3   520.

4 Geritz, S.A.H., Gyllenberg, M., Jacobs, F.J.A. and Parvinen, K. 2002. Invasion dynamics and
5   attractor inheritance. *J. Math. Biol.*, **44**: 548-560.

6 Geritz, S.A.H., Metz, J.A.J., Kisdi, É. and Meszéna, G. 1997. Dynamics of adaptation and
7   evolutionary branching. *Phys. Rev. Lett.*, **78**: 2024-2027.

8 Geritz, S.A.H., Kisdi, É., Meszéna, G. and Metz, J.A.J. 1998. Evolutionarily singular strate-
9   gies and the adaptive growth and branching of the evolutionary tree. *Evol. Ecol.*, **12**: 35-
10   57.

11 Grant, B.R. and Grant, P. 2008. How and Why Species Multiply: The Radiation of Darwin's
12   Finches (Princeton Series in Evolutionary Biology), Princeton University Press

13 Heinz, S.K., Mazzucco, R. and Dieckmann, U. 2009. Speciation and the evolution of dispersal
14   along environmental gradients. *Evol. Ecol.*, **23**: 53-70.

15 Hendry, A.P. and Kinnison, M.T. 1999. The pace of modern life: measuring rates of contem-
16   porary microevolution. *Evolution*, **53**: 1637-1653.

17 Ito, H.C. and Dieckmann, U. 2007. A new mechanism for recurrent adaptive radiations. *Am.
18   Nat.*, **170**: E96-E111.

19 Ito, H.C. and Dieckmann, U. (submitted). Evolutionary branching under slow directional evo-
20   lution.

21 Ito, H.C. and Ikegami, T. 2006. Food web formation through recursive evolutionary branch-
22   ing. *J. Theor. Biol.*, **238**: 1-10.

23 Ito, H.C. and Shimada, M. 2007. Niche expansion: coupled evolutionary branching of niche
24   position and width. *Evol. Ecol. Res.*, **9**: 675-695.

25 Ito, H.C., Shimada, M. and Ikegami, T. 2009. Coevolutionary dynamics of adaptive radiation
26   for food-web development. *Popul. Ecol.*, **51**: 65-81.

27 Kisdi, É. and Geritz, S.A.H. 1999. Adaptive dynamics in allele space: evolution of genetic
28   polymorphism by small mutations in a heterogeneous environment. *Evolution*, **53**: 993-
29   1008.

1   Kinnison, M.T. and Hendry, A.P. 2001. The pace of modern life II: from rates of contempo-

2   rary microevolution to pattern and process. *Genetica*, **112-113**: 145-164.

3   Leimar, O. 2005. The evolution of phenotypic polymorphism: randomized strategies versus

4   evolutionary branching. *Am. Nat.*, **165**: 669-681.

5   Leimar, O. 2009. Multidimensional convergence stability. *Evol. Ecol. Res.*, **11**: 191-208.

6   Losos, J.B. 2009. Lizards in an Evolutionary Tree: Ecology and Adaptive Radiation of

7   Anoles. University of California Press, Berkeley, CA.

8   MacArthur, R. 1972. Geographical Ecology. Harper and Row, New York.

9   MacArthur, R. and Levins, R. 1967. The limiting similarity, convergence, and divergence of

10   coexisting species. *Am. Nat.*, **101**: 377-385.

11   Matessi, C. and Di Pasquale, C., 1996. Long term evolution of multi-locus traits. *J. Math.*

12   *Biol.*, **34**: 613-653.

13   Metz, J.A.J., Geritz, S.A.H., Meszéna, G., Jacobs, F.J.A. and van Heerwaarden, J.S. 1996.

14   Adaptive dynamics: a geometrical study of the consequences of nearly faithful reproduc-

15   tion. In: van Strien, S.J. and Verduyn-Lunel, S.M. (eds) Stochastic and Spatial Structures

16   of Dynamical Systems. North Holland, Amsterdam, The Netherlands, pp 183-231.

17   Metz, J.A.J., Nisbet, R.M. and Geritz, S.A.H. 1992. How should we define 'fitness' for gen-

18   eral ecological scenarios? *Trends Ecol. Evol.*, **7**: 198-202.

19   Payne, J.L., Mazzucco and R., Dieckmann, U. 2011. The evolution of conditional dispersal

20   and reproductive isolation along environmental gradients. *J. Theor. Biol.*, **273**: 147-155.

21   Ravigné, V., Dieckmann, U. and Olivieri, I. 2009. Live where you thrive: joint evolution of

22   habitat choice and local adaptation facilitates specialization and promotes diversity. *Am.*

23   *Nat.*, **174**: E141-E169.

24   Roughgarden, J. 1972. Evolution of niche width. *Am. Nat.*, **106**: 683-718.

25   Roughgarden, J. 1974. Species packing and the competition function with illustrations from

26   coral reef fish. *Theor. Popul. Biol.*, **5**: 163-186.

27   Roughgarden, J. 1976. Resource partitioning among competing species: a coevolutionary ap-

28   proach. *Theor. Popul. Biol.*, **9**: 388-424.

29   Schluter, D. 2000. The Ecology of Adaptive Radiation. Oxford University Press, Oxford.

1   Seehausen, O. 2006. African cichlid fish: a model system in adaptive radiation research. *Proc.*

2   *R. Soc. Lond. B*, **273**:1987-1998.

3   Vukics, A., Asboth, J. and Meszéna, G. 2003. Speciation in multivariate evolutionary space.

4   *Phys. Rev. E.*, **68**: 041903.

5   **FIGURE CAPTIONS**

6   **Figure 1.** Illustration of the local characteristics of an evolutionary-branching line. For check-

7   ing the conditions for an evolutionary-branching line (grey line), the trait space (X,Y)

8   (frame axes) is locally normalized so that in the new coordinates (x,y) (black lines) muta-

9   tional steps are isotropic and disruptive selection is maximal in the direction of x. If at a

10   phenotype $\mathbf{S}_0$ the maximum disruptive selection D_{xx} in the direction of x is sufficiently

11   strong compared to the directional selection G_y in the direction of y, and if $\mathbf{S}_0$ is moreover

12   convergence stable in the direction of x, then an evolutionary branching-line is passing

13   through $\mathbf{S}_0$.

14   **Figure 2.** Prediction and observation of evolutionary-branching lines and areas in a resource-

15   competition model with evolving bivariate niche positions and non-isotropic mutational steps.

16   (a) Predicted evolutionary-branching line, evolutionary-branching area, and 20%-threshold

17   area, depicted by a line segment and by two nested areas filled with dark and light colors, re-

18   spectively. The colors of the line and areas follow a red-blue gradation indicating the predict-

19   ed directions of evolutionary branching: pure red and pure blue correspond to evolutionary

20   branching in the directions of the X-axis and Y-axis, respectively. Gray arrows indicate the

21   directional evolution of monomorphic populations. The black and gray lines are zero-isoclines

22   of the fitness gradient in the directions of the traits X and Y, respectively. (b) Occurrences

23   of evolutionary branching (triangles) in numerically calculated evolutionary dynamics starting

24   from 200 phenotypes randomly chosen from a uniform distribution across the shown trait

25   space. Observed directions of evolutionary branching are indicated by the same colors as in

26   (a). To facilitate comparison, the dashed curve repeats the boundary of the 20%-threshold area

27   from (a). Two example trajectories of evolutionary dynamics are shown as dark-yellow and

1   green curves, respectively, with initial phenotypes marked by the letters 'c' and 'd.' These

2   marks match the panels on the right, showing evolutionary dynamics over time, with thick

3   and thin curves corresponding to the traits X and Y, respectively. Filled circles in (b) indi-

4   cate the final phenotypes shown in (c) and (d), while filled triangles in (b) indicate the pheno-

5   types at which evolutionary branching occurs in the two example trajectories. Parameters:

6     $\sigma_K = 0.8$, $\sigma_\alpha = 0.5$, $K_0 = 1000$, $\varepsilon_e = 10^{-5}$, $\mu = 10^{-5}$, $\sigma_1 = 0.01$, $\sigma_2 = 0.003$.

7   **Figure 3.** Prediction and observation of evolutionary-branching lines and areas in a resource-

8   competition model with evolving niche positions and widths. (a) Predicted evolutionary-

9   branching line (red line at the center bottom), evolutionary-branching areas (red and small

10   blue areas), and 20%-threshold areas (light-red and light-blue areas). Other elements are as in

11   Fig. 2a. The inset shows a magnified view of the evolutionary-branching areas and corre-

12   sponding 20%-threshold area around the evolutionary-branching point at $(X, Y) = (0, 0.282)$.

13   (b) Occurrences of evolutionary branching (triangles) in numerically calculated evolutionary

14   dynamics starting from 700 phenotypes randomly chosen from a uniform distribution across

15   the shown trait space. Two example trajectories of evolutionary dynamics are shown as in

16   Figs. 2b. Other elements are as in Fig. 2b. Parameters: $\sigma_R = 0.2$, $m_R = 60$, $R_0 = 400$,

17    $\lambda = 0.3$, $\alpha = \beta = \gamma = 1$, $d_0 = 0.1$, $d_1 = 0.5$, $\varepsilon_e = 10^{-5}$, $\mu = 10^{-5}$, $\sigma_X = 0.01$, $\sigma_Y = 0.003$

18   (α, β, and γ are introduced in Appendix D, while d_0 and d_1 are introduced in Appendix

19   E).

20   **Figure 4.** Prediction and observation of evolutionary-branching lines and areas in a predator-

21   prey model with evolving predator-niche and prey-niche positions. (a) Predicted evolutionary-

22   branching lines (red lines), evolutionary-branching areas (red areas), and 20%-threshold areas

23   (light-red areas). Other elements are as in Figs. 2a and 3a. (b) Occurrences of evolutionary

24   branching (triangles) in numerically calculated evolutionary dynamics starting from 200 phe-

25   notypes randomly chosen from a uniform distribution across the shown trait space. Two ex-

26   ample trajectories of evolutionary dynamics are shown as in Fig. 2b and 3b. Other elements

27   are as in Figs. 2b and 3b. Parameters: $\sigma_c = \sigma_r = 0.06$, $\sigma_R = 0.08$, $R_0 = 4000$, $m_R = 60$,

1    $\lambda = 0.3$, $\alpha = 5$, $\beta = \gamma = 1$, $d = 0.1$, $\varepsilon_e = 10^{-5}$, $\mu = 10^{-5}$, $\sigma_X = 0.003$, $\sigma_Y = 0.001$ (α, β,

2   and γ are introduced in Appendix D).

APPENDIX A: MUTATION PROBABILITY DISTRIBUTIONS

4   Here we explain how the mutation probability distributions used in our three examples are

5   defined and interpreted in terms of mutational step sizes. For all three examples, we define the

6   mutation probability distributions as bivariate normal distributions in the original coordinate

7   system $\mathbf{S} = (X, Y)^{\mathrm{T}}$,

8
$$M(\boldsymbol{\delta}\mathbf{S}) = \exp(-\tfrac{1}{2}\,\boldsymbol{\delta}\mathbf{S}^{\mathrm{T}}\,\boldsymbol{\Lambda}^{-1}\,\boldsymbol{\delta}\mathbf{S})/(2\pi\,\sqrt{\det\boldsymbol{\Lambda}})\,, \tag{A1a}$$

9   where $\boldsymbol{\Lambda}$ is the mutational variance-covariance matrix, given by

10
$$\boldsymbol{\Lambda} = \begin{pmatrix} \sigma_X^2 & \sigma_{XY}^2 \\ \sigma_{XY}^2 & \sigma_Y^2 \end{pmatrix} \iint \begin{pmatrix} X^2 & XY \\ XY & Y^2 \end{pmatrix} M(\mathbf{S})\,\mathrm{d}X\mathrm{d}Y\,. \tag{A1b}$$

11   The two eigenvalues of the symmetric matrix $\boldsymbol{\Lambda}$ are real and give the maximum and mini-

12   mum variances of mutational step sizes, and the two corresponding eigenvectors give the di-

13   rections in which these extrema are attained.

14   For the first model, $\boldsymbol{\Lambda}$ is given by

15
$$\boldsymbol{\Lambda} = \mathbf{P}_{\boldsymbol{\Lambda}}\begin{pmatrix} \sigma_1^2 & 0 \\ 0 & \sigma_2^2 \end{pmatrix}\mathbf{P}_{\boldsymbol{\Lambda}}^{-1}\,,$$
$$\mathbf{P}_{\boldsymbol{\Lambda}} = \frac{1}{\sqrt{2}}\begin{pmatrix} -1 & 1 \\ 1 & 1 \end{pmatrix} \quad \frac{1}{\sqrt{2}}(\mathbf{e}_1, \mathbf{e}_2)\,, \tag{A2}$$

16   with $\sigma_1 \geq \sigma_2 > 0$. Accordingly, the standard deviation of mutational step sizes has its maxi-

17   mum σ_1 in the direction of $\mathbf{e}_1 = (-1,1)^{\mathrm{T}}$, and its minimum σ_2 in the direction of

18    $\mathbf{e}_2 = (1,1)^{\mathrm{T}}$. For the second and third model, $\boldsymbol{\Lambda}$ is given by $((\sigma_X^2, 0), (0, \sigma_Y^2))^{\mathrm{T}}$, with

19    $\sigma_X \geq \sigma_Y > 0$.

APPENDIX B: CONDITIONS FOR PROTECTED DIMORPHISMS FOR DIS-

RUPTIVE SELECTION PARALLEL TO DIRECTIONAL SELECTION

3   Here we derive conditions for the emergence of protected dimorphisms along maximum-

4   likelihood-invasion paths (MLIPs) for settings in which the maximum disruptive selection is

5   parallel to directional selection in the locally normalized coordinate system. We first examine

6   which mutants in such settings create maximum-likelihood invasions (MLI mutants), which

7   then enables us to derive the aforementioned conditions.

8   We consider a locally normalized coordinate system $\mathbf{s} = (x, y)^{\mathrm{T}}$ with origin at $\mathbf{S}_0$, in

9   which akin to Eqs. (1) the normalized invasion-fitness function is expressed as

10
$$
\begin{aligned}
f(\mathbf{s}';\mathbf{s}) = {} & G_x \delta x + G_y \delta y \\
& + \frac{1}{2} C_{xx} x \delta x + \frac{1}{2} C_{yy} y \delta y + \frac{1}{2} C_{xy} x \delta y + \frac{1}{2} C_{yx} y \delta x \\
& + \frac{1}{2} D_{xx} \delta x^2 + \frac{1}{2} D_{yy} \delta y^2.
\end{aligned}
\tag{B1a}
$$

11   As before, we assume that $\mathbf{s}$ is under disruptive selection and that the strength of disruptive

12   selection is maximal along the x-axis ($D_{xx} > 0$).

13   We assume that the resident is located at the origin, $\mathbf{s} = (0,0)^{\mathrm{T}}$, corresponding to $\mathbf{S}_0$,

14   without loss of generality. Because directional selection is assumed to be parallel to the direc-

15   tion of maximum disruptive selection, we can infer that $G_y = 0$. Then, $x, y = 0$ and Eq.

16   (B1a) reduces to

17
$$
f(\mathbf{s}';\mathbf{s}) = G_x \delta x + \frac{1}{2} D_{xx} \delta x^2 + \frac{1}{2} D_{yy} \delta y^2.
\tag{B1b}
$$

18   According to Dieckmann and Law (1996) and Ito and Dieckmann (submitted), the probability

19   for mutant $\mathbf{s}'$ to invade resident $\mathbf{s}$ is given by

20
$$
P(\mathbf{s}';\mathbf{s}) = T \mu \hat{n} M(\delta\mathbf{s}) f(\mathbf{s}';\mathbf{s})_+,
\tag{B2a}
$$

21   where T is a normalization ensuring $\int P(\mathbf{s}';\mathbf{s}) \, \mathrm{d}\mathbf{s}' = 1$, and the subscript "+" indicates the

22   conversion of negative values h to 0. Below, we can omit this subscript since we focus on the

23   maximum of $P(\mathbf{s}';\mathbf{s})$, for which $f(\mathbf{s}';\mathbf{s})$ always is positive. In this normalized trait space,

24   the distribution $M(\delta\mathbf{s})$ of mutational steps $\delta\mathbf{s}$ is given by an isotropic bivariate normal

1   distribution, $M(\boldsymbol{\delta s}) = N(\delta x, 0, \sigma^2)N(\delta y, 0, \sigma^2)$. Substituting this and Eq. (B1b) into Eq.

2   (B2a) yields

3 $$P(\mathbf{s}';\mathbf{s}) = A\exp\left(-\frac{\delta x^2 + \delta y^2}{2\sigma^2}\right)\left[G_x\delta x + \frac{1}{2}D_{xx}\delta x^2 + \frac{1}{2}D_{yy}\delta y^2\right], \tag{B2b}$$

4   where $A = \mu\hat{n}T/(2\pi\sigma^2)$. The mutant with maximum likelihood of invasion (MLI mutant),

5   denoted by $\mathbf{s}'_{\mathrm{MLI}} = (x'_{\mathrm{MLI}}, y'_{\mathrm{MLI}})^{\mathrm{T}}$, maximizes $P(\mathbf{s}';\mathbf{s})$. The mutational step taken by the MLI

6   mutant is $\boldsymbol{\delta s}_{\mathrm{MLI}} = (\delta x_{\mathrm{MLI}}, \delta y_{\overline{\mathrm{MLI}}})^{\mathrm{T}} = \mathbf{s}'_{\mathrm{MLI}} - \mathbf{s}$. For convenience, we express mutational steps in

7   polar coordinate $(\delta x, \delta y)^{\mathrm{T}} = (\varepsilon\cos\theta, \varepsilon\sin\theta)^{\mathrm{T}}$, which yields

8
$$P(\mathbf{s}';\mathbf{s}) = A\exp\left(-\frac{\varepsilon^2}{2\sigma^2}\right)\left[G_x\varepsilon\cos\theta + \frac{1}{2}D_{xx}\varepsilon^2\cos^2\theta + \frac{1}{2}D_{yy}\varepsilon^2\sin^2\theta\right]$$
$$= A\exp\left(-\frac{\varepsilon^2}{2\sigma^2}\right)\left[\frac{1}{2}D_{yy}\varepsilon^2 + \frac{1}{2}(D_{xx} - D_{yy})\varepsilon^2\cos^2\theta + G_x\varepsilon\cos\theta\right]. \tag{B2c}$$

9   Notice that $D_{xx} - D_{yy} > 0$, because disruptive selection is maximal in the direction of x. As

10     $\cos\theta$ is maximal and minimal at $\theta = 0$ and $\theta = \pi$, respectively, while $\cos^2\theta$ is maximal

11   at $\theta = 0$ and $\theta = \pi$, the invasion probability above has is maximum at $\theta = 0$ for positive

12     $G_x\varepsilon$ and at $\theta = \pi$ for negative $G_x\varepsilon$. Thus, the MLI mutant fulfills $\delta y_{\mathrm{MLI}} = 0$ and δx_{MLI}

13   is given by the δx that maximizes

14 $$P(\mathbf{s}';\mathbf{s}) = A\exp\left(-\frac{\delta x^2}{2\sigma^2}\right)\left[G_x\delta x + \frac{1}{2}D_{xx}\delta x^2\right]. \tag{B2d}$$

15   The terms above are symmetric with respect to the sign of δx, except for $G_x\delta x$. Therefore,

16   when G_x is positive, $P(\mathbf{s}';\mathbf{s})$ for any negative δx is smaller than $P(\mathbf{s}';\mathbf{s})$ for a positive

17   δx with the same absolute value. Thus, $\delta x_{\mathrm{MLI}} > 0$ holds for $G_x > 0$. Analogously,

18     $\delta x_{\mathrm{MLI}} < 0$ holds for $G_x < 0$.

19   In addition, $\delta x = \delta x_{\mathrm{MLI}}$ has to fulfill

20 $$\frac{\partial P(\mathbf{s}';\mathbf{s})}{\partial\delta x} = A\frac{1}{\sigma^2}\exp\left(-\frac{\delta x^2}{2\sigma^2}\right)\left[G_x(\sigma^2 - \delta x^2) + \frac{1}{2}D_{xx}\delta x(2\sigma^2 - \delta x^2)\right] = 0. \tag{B3}$$

21   For positive G_x, this requires $\sigma \le \delta x_{\mathrm{MLI}} \le \sqrt{2}\sigma$ (because $D_{xx}\delta x_{\mathrm{MLI}} > 0$, as D_{xx} is as-

22   sumed to be positive and $\delta x_{\mathrm{MLI}} > 0$ for $G_x > 0$). For negative G_x, similarly,

1     $-\sqrt{2}\sigma \leq \delta x_{\mathrm{MLI}} \leq -\sigma$ is required (because then $D_{\mathrm{xx}}\delta x_{\mathrm{MLI}} < 0$). In summary, the MLI mutant

2   thus always fulfills $\sigma \leq |\delta x_{\mathrm{MLI}}| \leq \sqrt{2}\sigma$ and $\delta y_{\mathrm{MLI}} = 0$.

3   On the basis of these features of MLI mutants, we now examine whether the MLI mutant

4   and the considered resident can coexist. The conditions for protected dimorphism are given by

5   conditions for mutual invasiblity, $f(\mathbf{s}'_{\mathrm{MLI}};\mathbf{s}) > 0$ and $f(\mathbf{s};\mathbf{s}'_{\mathrm{MLI}}) > 0$. By substituting

6     $\mathbf{s}'_{\mathrm{MLI}} = (\delta x_{\mathrm{MLI}} + x, y)^{\mathrm{T}}$ and $x = y = 0$ into Eq. (B1a), these conditions are expressed as

$$f(\mathbf{s}'_{\mathrm{MLI}};\mathbf{s}) = G_{\mathrm{x}}\delta x_{\mathrm{MLI}} + \frac{1}{2}D_{\mathrm{xx}}\delta x_{\mathrm{MLI}}^{2} > 0, \tag{B4a}$$

8   and

$$f(\mathbf{s};\mathbf{s}'_{\mathrm{MLI}}) = \; G_{\mathrm{x}}\delta x_{\mathrm{MLI}} \quad \frac{1}{2}C_{\mathrm{xx}}\delta x_{\mathrm{MLI}}^{2} \quad \frac{1}{2}D_{\mathrm{xx}}\delta x_{\mathrm{MLI}}^{2} \quad 0. \tag{B4b}$$

10   If

$$C_{\mathrm{xx}} < 0, \tag{B5}$$

12   a sufficient condition for inequalities (B4) to be fulfilled is given by

$$\frac{|\delta x_{\mathrm{MLI}}|D_{\mathrm{xx}}}{2|G_{\mathrm{x}}|} > 1. \tag{B6}$$

14   As $\sigma \leq |\delta x_{\mathrm{MLI}}| \leq \sqrt{2}\sigma$, a sufficient condition for this inequality to be fulfilled is given by

$$\frac{\sigma D_{\mathrm{xx}}}{2|G_{\mathrm{x}}|} > 1. \tag{B7}$$

16   **APPENDIX C: IDENTIFYING EVOLUTIONARY-BRANCHING LINES AND**

17   **AREAS**

18   **General procedure**

19   Here we explain how to identify evolutionary-branching lines and areas in an arbitrary trait

20   space, according to Ito and Dieckmann (submitted). For checking conditions for evolutionary-

21   branching lines in an arbitrary trait space $\mathbf{S}$, the vector $\mathbf{G}$ and the matrices $\mathbf{C}$ and $\mathbf{D}$ of

22   the locally normalized invasion-fitness function $f(\mathbf{s}';\mathbf{s})$ are all that is needed. To obtain the-

se vector and matrices, the trait space $\mathbf{S}$ is first transformed so that mutational steps become isotropic, and then it is further rotated so that $\mathbf{D}$ becomes diagonal. Specifically, $F(\mathbf{S}';\mathbf{S})$ is approximated as the normalized invasion-fitness function, Eq. (1a),

$$F(\mathbf{S}';\mathbf{S}) = \breve{\mathbf{G}}\ \boldsymbol{\delta}\mathbf{S} + \frac{1}{2}(\mathbf{S} - \mathbf{S}_0)^{\mathrm{T}}\breve{\mathbf{C}}\ \boldsymbol{\delta}\mathbf{S} + \frac{1}{2}\boldsymbol{\delta}\mathbf{S}^{\mathrm{T}}\breve{\mathbf{D}}\ \boldsymbol{\delta}\mathbf{S},\qquad\text{(C1a)}$$

where

$$\begin{aligned}\breve{\mathbf{G}} &= \mathbf{F}_{\mathbf{S}'},\\ \breve{\mathbf{C}} &= \mathbf{F}_{\mathbf{S}'\mathbf{S}'} - \mathbf{F}_{\mathbf{S}\mathbf{S}} + \mathbf{F}_{\mathbf{S}\mathbf{S}'} - \mathbf{F}_{\mathbf{S}\mathbf{S}'}^{\mathrm{T}},\\ \breve{\mathbf{D}} &= \mathbf{F}_{\mathbf{S}'\mathbf{S}'},\end{aligned}\qquad\text{(C1b)}$$

with

$$\mathbf{F}_{\mathbf{S}'} = \begin{pmatrix} F_{\mathrm{X}'} & F_{\mathrm{Y}'} \end{pmatrix}_{\mathbf{S}'=\mathbf{S}=\mathbf{S}_0},$$

$$\mathbf{F}_{\mathbf{S}'\mathbf{S}'} = \begin{pmatrix} F_{\mathrm{X}'\mathrm{X}'} & F_{\mathrm{X}'\mathrm{Y}'} \\ F_{\mathrm{X}'\mathrm{Y}'} & F_{\mathrm{Y}'\mathrm{Y}'} \end{pmatrix}_{\mathbf{S}'=\mathbf{S}=\mathbf{S}_0},\ \mathbf{F}_{\mathbf{S}\mathbf{S}} \begin{pmatrix} F_{\mathrm{X}\mathrm{X}} & F_{\mathrm{X}\mathrm{Y}} \\ F_{\mathrm{X}\mathrm{Y}} & F_{\mathrm{Y}\mathrm{Y}} \end{pmatrix}_{\mathbf{S}'=\mathbf{S}\ \mathbf{S}_0},\ \mathbf{F}_{\mathbf{S}\mathbf{S}'} \begin{pmatrix} F_{\mathrm{X}\mathrm{X}'} & F_{\mathrm{X}\mathrm{Y}'} \\ F_{\mathrm{Y}\mathrm{X}'} & F_{\mathrm{Y}\mathrm{Y}'} \end{pmatrix}_{\mathbf{S}'\ \mathbf{S}\ \mathbf{S}_0},\qquad\text{(C1c)}$$

where F_{α} for $\alpha = \mathrm{X}',\mathrm{Y}',\mathrm{X},\mathrm{Y}$ and $F_{\alpha\beta}$ for $\alpha,\beta = \mathrm{X}',\mathrm{Y}',\mathrm{X},\mathrm{Y}$ denote the first and second partial derivatives of $F(\mathbf{S}';\mathbf{S})$ with respect to α and β, respectively.

By locally normalizing the trait space through an affine transformation, i.e., by substituting $\mathbf{S} - \mathbf{S}_0 = \mathbf{Q}^{\mathrm{T}}\mathbf{B}\mathbf{s}$ and $\boldsymbol{\delta}\mathbf{S} = \mathbf{Q}^{\mathrm{T}}\mathbf{B}\ \boldsymbol{\delta}\mathbf{s}$ into Eq. (C1a) and comparing with Eq. (1a), we see that $\mathbf{G}$, $\mathbf{C}$ and $\mathbf{D}$ are given by

$$\begin{aligned}\mathbf{G} &= \breve{\mathbf{G}}\mathbf{Q}^{\mathrm{T}}\mathbf{B},\\ \mathbf{C} &= \mathbf{B}^{\mathrm{T}}\mathbf{Q}\breve{\mathbf{C}}\mathbf{Q}^{\mathrm{T}}\mathbf{B},\\ \mathbf{D} &= \mathbf{B}^{\mathrm{T}}\mathbf{Q}\breve{\mathbf{D}}\mathbf{Q}^{\mathrm{T}}\mathbf{B}.\end{aligned}\qquad\text{(C2a)}$$

The matrix $\mathbf{Q}$ describes the scaling of mutational step sizes to make them isotropic,

$$\mathbf{Q} = \frac{1}{\sigma}\begin{pmatrix} \sigma_{\mathrm{X}} & \sigma_{\mathrm{XY}}^2/\sigma_{\mathrm{X}} \\ 0 & \sqrt{\sigma_{\mathrm{X}}^2\sigma_{\mathrm{Y}}^2 - \sigma_{\mathrm{XY}}^4}/\sigma_{\mathrm{X}} \end{pmatrix},\qquad\text{(C2b)}$$

where σ_{X}^2, σ_{Y}^2, and σ_{XY}^2 are the components of the mutational variance-covariance matrix $\boldsymbol{\Lambda}$, and σ^2 is the dominant eigenvalue of $\boldsymbol{\Lambda}$, measuring the maximum variance of mutational step sizes among all directions in trait spaces. The matrix $\mathbf{Q}$ can be obtained as the

1   Cholesky decomposition of $\mathbf{\Lambda}/\sigma^2$, $\mathbf{\Lambda}/\sigma^2 = \mathbf{Q}^{\mathrm{T}}\mathbf{Q}$, with $\mathbf{Q}$ having upper-triangular form.

2   The matrix $\mathbf{B}$ describes the rotation of the trait axes to align them with the direction of max-

3   imum disruptive selection,

4 $$\mathbf{B} = (\mathbf{v}_1, \mathbf{v}_2), \tag{C2c}$$

5   where $\mathbf{v}_1$ and $\mathbf{v}_2$ are the eigenvectors of $\mathbf{Q}\breve{\mathbf{D}}\mathbf{Q}^{\mathrm{T}}$, ordered so that the corresponding eigen-

6   values fulfill $\lambda_1 > \lambda_2$, which makes $\mathbf{D}$ diagonal with $D_{\mathrm{xx}} > D_{\mathrm{yy}}$.

7   By substituting Eqs. (C2) into the conditions for evolutionary-branching lines, Eqs. (2a-c),

8   the set of phenotypes $\mathbf{S}_0$ fulfilling those conditions is found, thus yielding the evolutionary-

9   branching lines.

10 **Illustrative example**

11   Here we elaborate on the illustrative analysis of evolutionary-branching lines and areas

12   around an evolutionary-branching point in the simple example briefly explained in the subsec-

13   tion "Sizes and shapes of evolutionary-branching lines and areas" in the main text.

14   As explained there, we suppose that a trait space $\mathbf{S} = (X, Y)^{\mathrm{T}}$ possesses an evolutionary-

15   branching point at its origin. For a point $\mathbf{S}_0$ close to the origin, the invasion-fitness function

16     $F(\mathbf{S}'; \mathbf{S})$ can be expanded as shown in Eq. (C1a). By further expanding $\breve{\mathbf{G}}$, $\breve{\mathbf{C}}$, and $\breve{\mathbf{D}}$ in

17   terms of $\mathbf{S}_0$ around the origin, these are approximately given by

18 $$\breve{\mathbf{G}} = \breve{\tilde{\mathbf{G}}}\ \mathbf{S}_0^{\mathrm{T}}\breve{\tilde{\mathbf{C}}}, \quad \breve{\mathbf{C}}\ \breve{\tilde{\mathbf{C}}}, \quad \text{and} \quad \breve{\mathbf{D}}\ \breve{\tilde{\mathbf{D}}}, \tag{C3}$$

19   where $\breve{\tilde{\mathbf{G}}}$, $\breve{\tilde{\mathbf{C}}}$, and $\breve{\tilde{\mathbf{D}}}$ denote the matrices $\breve{\mathbf{G}}$, $\breve{\mathbf{C}}$, and $\breve{\mathbf{D}}$ at $\mathbf{S}_0 = (0,0)^{\mathrm{T}}$, respectively.

20   For the origin to be an evolutionarily singular point, $\breve{\tilde{\mathbf{G}}} = \mathbf{0}$ is required. For the sake of illus-

21   tration, we assume that $\breve{\tilde{\mathbf{D}}} = ((D_{\mathrm{XX}}, 0), (0, D_{\mathrm{YY}}))^{\mathrm{T}}$, $D_{\mathrm{XX}} \geq D_{\mathrm{YY}}$, and $\breve{\tilde{\mathbf{C}}} = ((C_{\mathrm{XX}}, 0), (0, C_{\mathrm{YY}}))^{\mathrm{T}}$.

22   And for the origin to be an evolutionary-branching point, we assume that it is strongly con-

23   vergence stable, $C_{\mathrm{XX}}, C_{\mathrm{YY}} < 0$, and that it is not evolutionarily stable, $D_{\mathrm{XX}} > 0$. In addition,

24   we assume that mutational steps in the traits X and Y have no correlation, $\sigma_{\mathrm{XY}} = 0$, and

25   are largest along the X-axis, $\sigma_{\mathrm{X}} \geq \sigma_{\mathrm{Y}}$. Then, the matrices $\mathbf{Q}$ and $\mathbf{B}$ are given by the

26   constant matrices,

1 $$\mathbf{Q} = \begin{pmatrix} 1 & 0 \\ 0 & \sigma_Y / \sigma_X \end{pmatrix} \quad \text{and} \quad \mathbf{B} \begin{pmatrix} 1 & 0 \\ 0 & 1 \end{pmatrix}, \tag{C4}$$

2 with $\sigma = \sigma_X$. Substituting Eqs. (C3) and (C4) into Eqs. (C2a) yields

3
$$\mathbf{G} = (G_x \quad G_y) = (C_{XX}X_0 \quad rC_{YY}Y_0),$$
$$\mathbf{C} = \begin{pmatrix} C_{xx} & C_{xy} \\ C_{yx} & C_{yy} \end{pmatrix} = \begin{pmatrix} C_{XX} & 0 \\ 0 & r^2 C_{YY} \end{pmatrix}, \tag{C5}$$
$$\mathbf{D} = \begin{pmatrix} D_{xx} & D_{xy} \\ D_{xy} & D_{yy} \end{pmatrix} \begin{pmatrix} D_{XX} & 0 \\ 0 & r^2 D_{YY} \end{pmatrix},$$

4 with $r = \sigma_Y / \sigma_X$. Substituting Eqs. (C5) into the conditions for evolutionary-branching lines

5 and areas, Eqs. (2) and (3a), then yields Eqs. (4) and (5).

6 **APPENDIX D: FUNCTIONAL RESPONSE IN SECOND AND THIRD MOD-**

7 **ELS**

8 Here we explain how the functional response used in the second and third model is derived.

9 Extending results by Beddington (1975) and DeAngelis *et al.* (1975), we start by deriving the

10 functional response of phenotype $\mathbf{S}$ to resource type z,

11
$$g_R(z,\mathbf{S}) = \phi(\mathbf{S})Ac(z,\mathbf{S})e_R R(z), \tag{D1a}$$

12 where $\phi(\mathbf{S})$ is the search effort per consumption effort, A is the total rate of consumption

13 effort, and $c(z,\mathbf{S})$ describes the probability density of consumption effort over resources

14 types z by phenotype $\mathbf{S}$ per unit of its biomass. Thus, $\phi(\mathbf{S})Ac(z,\mathbf{S})$ is the probability

15 density of search effort per unit time invested on resource type z by phenotype $\mathbf{S}$ per unit

16 of its biomass (search effort for short). As a first-order approximation, the encounter rate of

17 phenotype $\mathbf{S}$ with resource type z is assumed to be proportional to this search effort and to

18 the density $R(z)$ of resource type z, resulting in the proportionality constant e_R.

19   The first-order approximation is also applied to the rate of interference competition expe-

20 rienced by phenotype $\mathbf{S}$ while consuming resource type z,

21
$$g_C(z,\mathbf{S}) = \phi(\mathbf{S})Ac(z,\mathbf{S})e_C C(z), \tag{D1b}$$

1 which is thus assumed to be proportional to the search effort and to the total consumption

2 effort $C(z)$ invested on resource type z by all phenotypes, with a proportionality constant

3 e_C. $C(z)$ is given by

$$C(z) = A \sum_{j=1}^{L} n_j c(z, \mathbf{S}_j) . \tag{D2}$$

5 The sum of energy invested into resource search, resource handling, and interference

6 competition, measured in terms of rates and integrated over all resource types z, equals the

7 total rate A of consumption effort,

$$\int \phi(\mathbf{S}) A c(z, \mathbf{S}) \, \mathrm{d}z + \int h_R g_R(z, \mathbf{S}) \, \mathrm{d}z + \int h_C g_C(z, \mathbf{S}) \, \mathrm{d}z = A , \tag{D3}$$

9 where h_R and h_C scale the energy requirements for resource handling and interference

10 competition relative to those for resource search. Here it is assumed that these relative energy

11 requirements do not depend on resource type, and that they are not complicated by spatial

12 population structure. Substituting Eqs. (D1) into Eq. (D2) yields

$$\phi(\mathbf{S}) = \frac{1}{1 + h_R e_R \tilde{R}(\mathbf{S}) + h_C e_C \tilde{C}(\mathbf{S})} , \tag{D4}$$

14 and substituting this into Eq. (D1a) yields

$$g_R(z, \mathbf{S}) = \frac{A c(z, \mathbf{S}) R(z)}{\alpha + \beta \tilde{R}(\mathbf{S}) + \gamma \tilde{C}(\mathbf{S})} , \tag{D5}$$

16 where

$$\tilde{R}(\mathbf{S}) = \int c(z, \mathbf{S}) R(z) \, \mathrm{d}z , \quad \tilde{C}(\mathbf{S}) = \int c(z, \mathbf{S}) C(z) \, \mathrm{d}z , \tag{D6}$$

18 $\alpha = 1/e_R$, $\beta = h_R$, and $\gamma = h_C e_C / e_R$. Integrating Eq. (D4) over all resource types z,

19 $g(\mathbf{S}) = \int g_R(z, \mathbf{S}) \, \mathrm{d}z$, finally yields the sought functional response,

$$g(\mathbf{S}) = \frac{A \tilde{R}(\mathbf{S})}{\alpha + \beta \tilde{R}(\mathbf{S}) + \gamma \tilde{C}(\mathbf{S})} . \tag{D7}$$

21 Here the parameters α, β, and γ measure, respectively, the costs for resource search,

22 resource handling, and interference competition.

APPENDIX E: INVASION FITNESS IN SECOND MODEL

Here we derive the invasion-fitness function for the second model. First, for the functional response in Eq. (D7) we need to specify the total amounts of resource and competitors encountered by phenotype $\mathbf{S}_i$, $\tilde{R}(\mathbf{S}_i)$ and $\tilde{C}(\mathbf{S}_i)$, which according to Eq. (D6) are given by the following overlap integrals,

$$\tilde{R}(\mathbf{S}_i) = \int c(z,\mathbf{S}_i)R(z)\,\mathrm{d}z = R_0\mathrm{N}(X_i,m_\mathrm{R},Y_i^2 + \sigma_\mathrm{R}^2),$$
$$\tilde{C}(\mathbf{S}_i) = \int c(z,\mathbf{S}_i)C(z)\,\mathrm{d}z = A\sum\nolimits_{j=1}^{L} n_j\mathrm{N}(X_i,X_j,Y_i^2 + Y_j^2),$$

(E1)

where $C(z)$ is the total consumption effort invested on resource type z by all phenotypes $\mathbf{S}_j$, as given by Eq. (D2).

Second, we describe the costs of specialization or generalization by an additional death rate that linearly varies with the niche width Y of a phenotype $\mathbf{S}$,

$$d(Y) = d_0 - d_1 Y,$$

(E2)

as specified by the two parameters d_0 and d_1: a positive d_1 results in a cost of specialization, whereas a negative d_1 results in a cost of generalization.

Third, for a monomorphic population with phenotype $\mathbf{S}$ and equilibrium biomass $\hat{n}$, the invasion fitness of a mutant with phenotype $\mathbf{S}'$ is then derived according to Eq. (7c) as

$$F(\mathbf{S}';\mathbf{S}) = \lim_{n' \to 0} \frac{1}{n'}\frac{\mathrm{d}n'}{\mathrm{d}t} = \lambda g(\mathbf{S}') - d(Y'),$$

(E3a)

with $g(\mathbf{S}')$ as specified in Eq. (D7) with

$$\tilde{R}(\mathbf{S}') = R_0\mathrm{N}(X',m_\mathrm{R},Y'^2 + \sigma_R^2),$$
$$\tilde{C}(\mathbf{S}') = A\hat{n}\mathrm{N}(X',X,Y'^2 + Y^2).$$

(E3b)

APPENDIX F: INVASION FITNESS IN THIRD MODEL

Here we derive the invasion-fitness function for the third model. First, the total resource distribution is given by

$$R(z) = B(z) + \sum\nolimits_{j=1}^{L} n_j r(z,\mathbf{S}_j).$$

(F1a)

1 The rate of actual resource gain by phenotype $\mathbf{S}_i$ is then given by $g(\mathbf{S}_i)$ as specified in Eq.

2 (D7) with

$$\tilde{R}(\mathbf{S}_i) = \int c(z,\mathbf{S}_i) R(z)\, dz = R_0 N(X_i, m_R, \sigma_c^2 + \sigma_R^2) + \sum_{j=1}^{L} n_j N(X_i, Y_j, \sigma_c^2 + \sigma_r^2),$$
$$\tilde{C}(\mathbf{S}_i) = \int c(z,\mathbf{S}_i) C(z)\, dz \quad A\sum_{j=1}^{L} n_j N(X_i, X_j, \sigma_c^2), \tag{F1b}$$

4 according to Eq. (D6), where $C(z)$ is the total consumption effort invested on resource type

5 z by all phenotypes $\mathbf{S}_j$, as given by Eq. (D2) By assuming that predators do not distinguish

6 phenotypes of prey when they share a same resource quality z, we obtain the functional

7 response of phenotype $\mathbf{S}_i$ to $\mathbf{S}_j$ as $g(\mathbf{S}_i)$ multiplied by the fraction of $\mathbf{S}_j$ in the re-

8 sources preyed upon by $\mathbf{S}_i$,

$$g_p(\mathbf{S}_i, \mathbf{S}_j) = g(\mathbf{S}_i) \int c(z,\mathbf{S}_i) n_j r(z,\mathbf{S}_j)\, dz / \tilde{R}(\mathbf{S}_i) \quad g(\mathbf{S}_i) n_j N(X_i, Y_j, \sigma_c^2 \quad \sigma_r^2) / \tilde{R}(\mathbf{S}_i). \tag{F1c}$$

10 Second, the rate of biomass loss of phenotype $\mathbf{S}_i$ per its unit biomass is then given by

$$l(\mathbf{S}_i) = \frac{1}{n_i} \sum_{j=1}^{L} n_j g_p(\mathbf{S}_j, \mathbf{S}_i) \tag{F2}$$

12 Third, for a monomorphic population with phenotype $\mathbf{S}$ and equilibrium biomass $\hat{n}$, the

13 invasion fitness of a mutant phenotype $\mathbf{S}'$ is then derived according to Eq. (8c) as

$$F(\mathbf{S}'; \mathbf{S}) = \lim_{n' \to 0} \frac{1}{n'} \frac{dn'}{dt} = \lambda g(\mathbf{S}') - g_p(\mathbf{S}, \mathbf{S}') - d, \tag{F3a}$$

15 with

$$\tilde{R}(\mathbf{S}') = N(X', m_R, \sigma_c^2 + \sigma_R^2) + \hat{n} N(X', Y, \sigma_c^2 + \sigma_r^2),$$
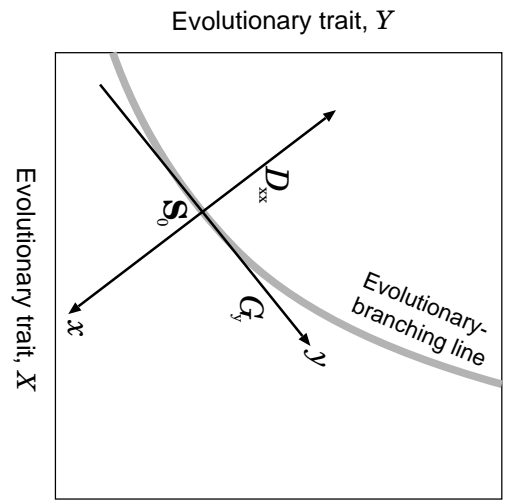$$\tilde{C}(\mathbf{S}') = A\hat{n} N(X', X, \sigma_c^2). \tag{F3b}$$

Figure 1

Figure 2

(a) Prediction
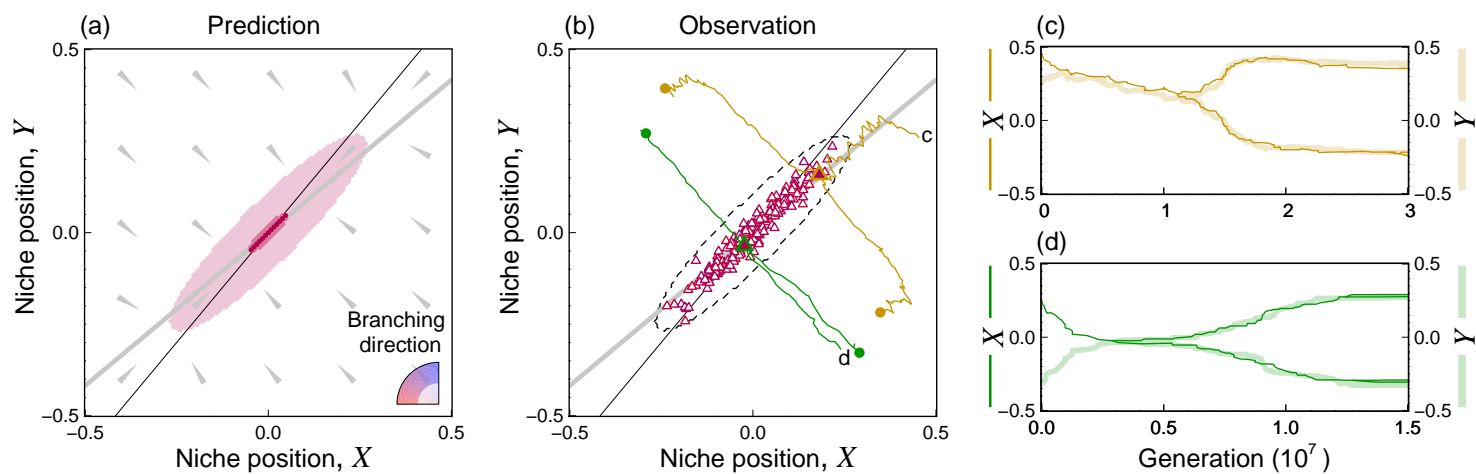(b) Observation
(c)
(d)

Figure 3

(a) Prediction
(b) Observation
(c)
(d)

Figure 4

(a) Prediction
(b) Observation
(c)
(d)